1997

The Interaction of Naphthoquinones With the Calcium Release Channel of Skeletal Muscle Sarcoplasmic Reticulum

Ruohong Xia
Portland State University

THESIS APPROVAL

The abstract and thesis of Ruohong Xia for the Master of Science in Physics were presented July 10, 1997, and accepted by the thesis committee and the department.

COMMITTEE APPROVALS: [redacted]

Jonathan J. Abramson, Chair

[redacted]

Pavel Smejtek

[redacted]

Carl C. Wamser
Representative of the Office of Graduate Studies

DEPARTMENT APPROVAL: [redacted]

Erik Bodegom, Chair
Department of Physics

* *

ACCEPTED FOR PORTLAND STATE UNIVERSITY BY THE LIBRARY

by [redacted] on 9/19/97

ABSTRACT

An abstract of the thesis of Ruohong Xia for the Master of Science in Physics in Physics presented July 10, 1997.

Title: The Interaction of Naphthoquinones with the Calcium Release Channel of Skeletal Muscle Sarcoplasmic Reticulum

The sarcoplasmic reticulum (SR) is an intracellular membrane system which regulates cytoplasmic calcium concentration in muscle and controls the contractile state of muscle. In this thesis, the interaction between naphthoquinone and the Ca^{2+} release mechanism of SR is described. 1,4-naphthoquinone (1,4NQ) is shown to stimulate Ca^{2+} release and to modify high-affinity ryanodine binding to skeletal muscle sarcoplasmic reticulum. The interaction between 1,4NQ and the SR involves the oxidation of critical sulfhydryl groups associated with the Ca^{2+} release mechanism. The modulation of ryanodine binding by 1,4NQ is biphasic. At low concentrations of 1,4NQ (<10 μM) ryanodine binding is stimulated, while at high concentrations (>10 μM) an inhibition of the ryanodine receptor (RyR) is observed. These studies reveal important characteristics of the RyR. There are at least two classes of functionally significant thiols associated with the RyR/Ca^{2+} release channel.

Oxidation of thiols induced by low concentrations of 1,4NQ activates the Ca^{2+} release mechanism. At higher concentrations of 1,4NQ, oxidation of a second class of thiols inactivates the ryanodine receptor. A model is presented in which oxidation of reaction thiols leads to the opening of the Ca^{2+} release channel, while oxidation of a second set of thiols results in closure of the Ca^{2+} release channel.

THE INTERACTION OF NAPHTHOQUINONES WITH THE CALCIUM RELEASE CHANNEL OF SKELETAL MUSCLE SARCOPLASMIC RETICULUM

BY

RUOHONG XIA

A thesis submitted in partial fulfillment of
the requirements for the degree of

MASTER OF SCIENCE

in

PHYSICS

Portland State University
1997

ACKNOWLEDGMENTS

I would like to extend my sincere appreciation and thanks to all the people who have assisted me in the completion of this thesis.

First of all, I would like to thank my advisor, Professor Jonathan J. Abramson, for his great guidance and supports in every stage of this project. Without his patience, understanding and encouragement, this project would not have been possible. Warm thanks also go to each member of the committee, Professor Pavel Smejtek, and Professor Carl C. Wamser, for their inspiration and support in this project.

I am also deeply indebted to the entire "Abramson Lab", Lisa, Shawn, Alex, and all the others who provided so much help to me in many ways. I enjoyed working with them in the unforgettable lab experiences.

I especially want to express my great debt to my colleague and good friend, Lisa Gnall, for her patience and tireless help in reading this manuscript as well as her valuable advice in the preparation of this thesis.

I also want to thank Dr. Erik Bodegom and the Physics Department for the encouraging help and support in these two unforgettable years.

Finally, my sincere appreciation and gratitude goes to my family in China, especially to my husband, Pei Huang, and my dear little son Haili. Their love and care, understanding and encouragement are the inspiration for my work, and they are always with me.

CONTENTS

LIST OF TABLES

LIST OF FIGURES

CHAPTER I

THE CALCIUM RELEASE CHANNEL

1 INTRODUCTION

Calcium is the most abundant cation in vertebrates. The human body contains 20-30 g of calcium per kg body weight (Affolter et al., 1980). The largest part of the body's Ca^{2+} is stored in the bones. Most intracellular organelles are known to contain Ca^{2+} in concentrations largely exceeding that of the cytosol. Unlike bones, where the same Ca^{2+} pool plays both a structural and a dynamic role, the various cellular Ca^{2+} stores have very different functions, and their dynamic relationships with either cytosolic or extracellular Ca^{2+} are extremely diversified. Calcium plays an important role in many biological processes, and is often referred to as a "second messenger". Calcium ions are involved in the control of enzyme activity, secretion, neurotransmitter release, cellular communication, and muscle contraction.

Muscle movement is regulated by the intracellular Ca^{2+} levels. The functional organic modulation of Ca^{2+} mobility, and the resulting generation of force is performed by a net-like structure, the sarcoplasmic reticulum (SR), which is a large localized Ca^{2+} pool in the muscle. After the muscle cell is stimulated by the attached neuron, depolarization of the transverse tubules (T-tubules) activates the dihydropyridine receptor (DHPR). This initiates a signal that is transmitted to the Ca^{2+} release channel (RyR), causing it to open. A rapid efflux of the Ca^{2+} from the SR causes an increase in the cytosolic Ca^{2+} concentration. Troponin then binds Ca^{2+}, and muscle contraction occurs. When the intracellular Ca^{2+} level falls again as it is pumped out of the cytosol, bound Ca^{2+} dissociates from troponin and the muscle relaxes. It is well known that the protein responsible for actively accumulating Ca^{2+} into the SR is the Ca^{2+}-Mg^{2+}-ATPase, a 110 kDa transmembrane protein. In contrast, the mechanism underlying Ca^{2+} release is still poorly understood.

The goal of this thesis is to describe the mechanism by which naphthoquinones interacts with the Ca^{2+} release channel of rabbit skeletal muscle sarcoplasmic reticulum.

2 MUSCLE AND CONTRACTION

2.1 Morphology of the Muscle

Vertebrate muscle can be classified into three types: skeletal, smooth and cardiac. Muscles have the ability to contract - that is, to exert a force when they are stimulated. A whole muscle is covered by a connective tissue sheath, called the

epimysium. Beneath the epimysium each skeletal muscle consists of many muscle fibers arranged in bundles called fasciculi. Each bundle, or fasciculus, is surrounded by a connective tissue sheath, called the perimusium. Each individual fiber, or cell, is surrounded by a thin, transparent membrane known as the sarcolemma (SL). Within the sarcolemma are the fluid protoplasma, or sarcoplasm, and hundreds to thousands of highly developed myofibrils, which run the length of the fiber parallel to each other. Similar to the muscle cell, which consists of many myofibrils, each myofibril consists of many still smaller myofilaments. Within the intracellular fluid, or cytoplasm, are found numerous mitochondria and nuclei (Fig.1), and the highly organized SR, with a structure similar to the endoplasmic reticulum (ER) of other cells.

The myofibrils exhibit alternating light and dark bands, giving the fiber its striated appearance. These striations are well defined when viewed under the microscope, and can be differentiated into several bands, zones, and lines associated with each sarcomere (Fig. 2). The Z-lines are composed of several filamentous proteins and the space between two adjacent Z-lines, about 2μm in a resting muscle, is the sarcomere. Within the sarcomere, the broad A-band is the region of overlap between the actin and myosin filaments (Fig. 2A). The region near the Z-line, in which only actin filaments are present, appears lighter under the microscope, and is called the I-band. Both actin and myosin filaments are present in the A-band, except in the H-zone in the center, where the filaments do not overlap in a the moysin, partially obliterating the H-zone.

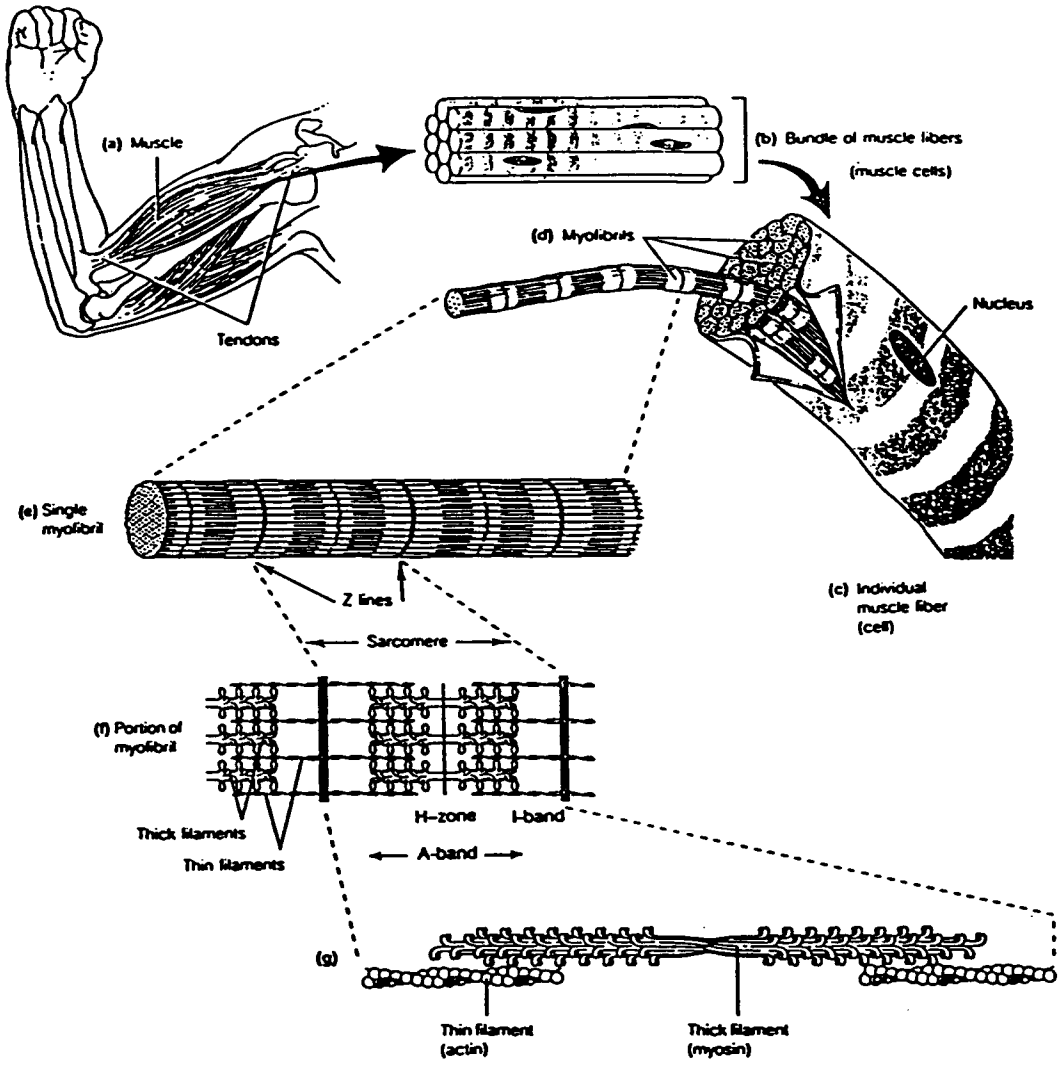

Figure 1. Levels of organization of skeletal muscle tissue. (a) Muscle tissue is attached by means of tendons to the specific bones it must move. (b) The tissue consists of muscle fibers, each of which is a long, thin multinucleate cell (c). (d) Within each cell are many myofibrils. (e) Each myofibril consists of bundles of filaments aligned laterally to give the skeletal muscle its striated appearance. (f) Within the myofibril, thick filaments interdigitate with thin filaments that are attached to the Z line. The unit of contraction along each myofibril is the sarcomere, defined as the distance from one Z line to the next. (g) The thick and thin filaments consist primarily of myosin and actin, respectively. (From Veot and Veot)

In the sliding filament model of contraction, as the filaments slide together, the Z-lines are brought closer to one another. Sliding of myofilaments is produced by the ratchetting action of numerous cross bridges that extend outward from myosin toward actin. These cross bridges are part of the myosin proteins that extend from the axis ofthe thick myofilaments to form "arms" that terminate in a globular "head" (Fig.3). The orientation of the cross bridges on one side of a sarcomere is opposite to that of the cross bridges on the other side, so that when the myosin cross bridges attach to the actin on each side of the sarcomere, they can pull the actin from each side toward the center. The myosin heads are bound to specific attachment sites on each of the actin subunits. When myosin binds to actin, they undergo a conformational change. This results in a power stroke. The thin filament is pulled toward the center of the A-band, and ATP is hydrolyzed by the myosin ATPase. Contraction is completed now.

Ca^{2+} plays a significant role in the attachment of the myosin heads to actin. The thin filament contains three types of proteins: actin, tropomyosin, and troponin. At low Ca^{2+} concentrations ($< 10^{-7}$ M), calcium does not bind to troponin, and tropomyosin prevents myosin from binding to actin, thereby maintaining the muscle in the relaxed state. At higher concentrations ($> 10^{-6}$ M), calcium binds to the C-subunit of troponin, inducing a conformational change that is transmitted to tropomyosin. The tropomyosin moves to the center of the thin filament, allowing the myosin head to attach to actin, thereby triggering contraction (Fig 4).

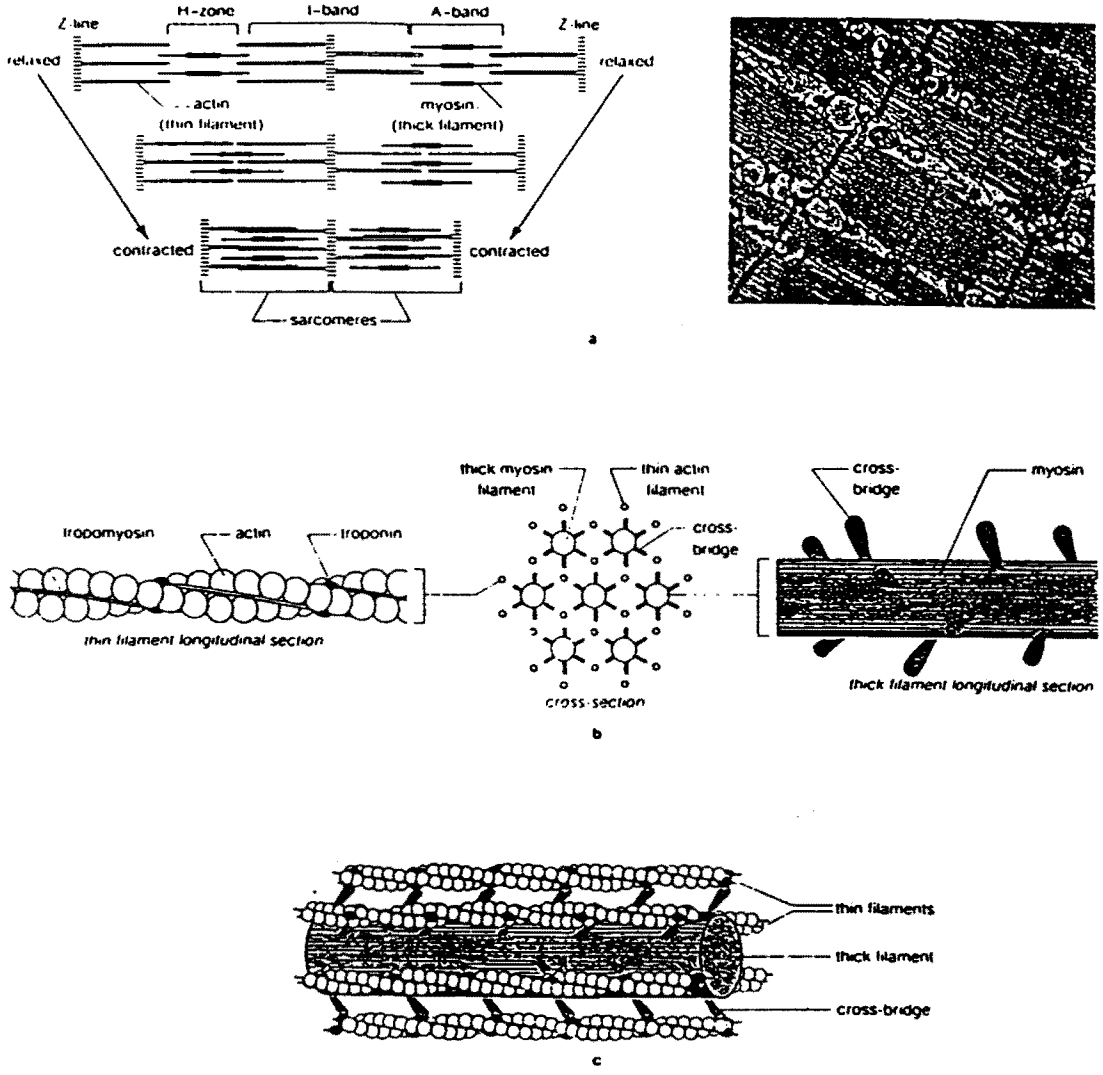

Figure 2. The arrangement of filaments in a sarcomere: (a) A schematic of the change in the arrangement of filaments from the relaxed to the contracted state, and a photomicrograph of the filaments. (b) The structure and arrangement of filaments. (c) Interaction between actin and myosin. (From Veot and Veot)

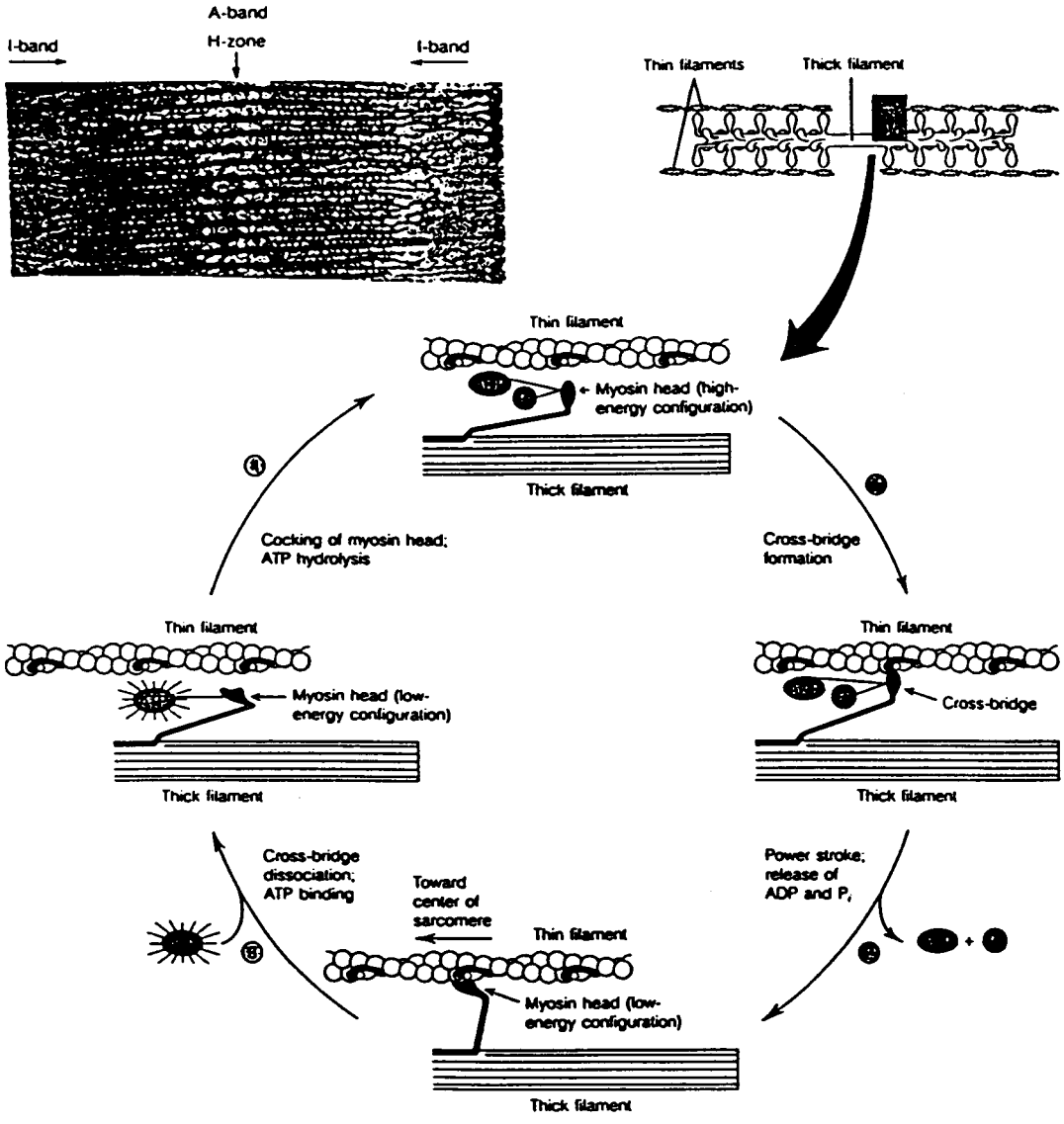

Figure 3. The cyclic process of muscle contraction. A small segment of adjacent thick and thin filaments (see inset) is used to illustrate the series of events whereby the cross-bridge formed by a myosin head is used to draw the thin filament toward the center of the sarcomere, thereby causing the myofibril to contract. The configuration shown at the top of the figure is that of relaxed muscle. When a muscle's fully contracted, its cross-bridges have the configuration shown at the bottom of the figure. (From Veot and Veot)

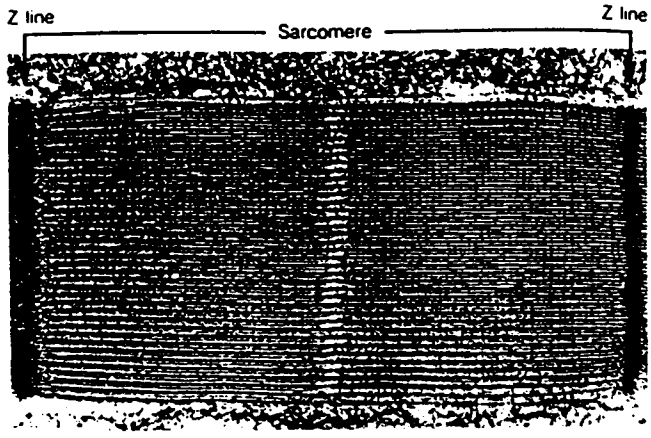

Figure 4. Cross-Bridges. The cross-bridges between thick and thin filaments formed by the projecting heads of myosin molecules can be readily seen in this electron micrograph of a single contracted sarcomere from a flight muscle of *Drosophila melanogaster*. A section of 0.5μm was photographed in a high-voltage electron microscope (24,500×) (From Lubert Stryer)

2.2 Calcium Regulation System of Muscle

2.2.1 *Excitation - Contraction Coupling model*

In the muscle cell, each myofibril is surrounded by the SR membrane. Adjacent to the SR are the T-tubules, which are extensions of the plasma membrane and penetrate deeply into each muscle fiber. The T-tubule is located at the junctions of the A- and I-bands in mammalian skeletal muscle. It runs perpendicular to both the myofibrils and the SR. The T-tubules rapidly carry an electrical signal in the form of an action potential into the interior of the cell to the SR system, so that each myofibril can respond quickly to the action potential.

Excitation-contraction (EC) coupling refers to the process in which action potentials propagated along the T-tubules are coupled to the release of Ca^{2+} from the

sarcoplasmic reticulum. At the triadic junction, the electrical signal in the T-tubule triggers rapid Ca^{2+} release from the SR. The resulting rise in myoplasmic calcium allows contraction to occur. Coupling between T-tubule depolarization and Ca^{2+} release from SR is believed to occur at the junction between the T-tubule and the SR membrane. At the protein level, the dihydrophridine receptor (DHPR) senses the action potential, and somehow communicates with the ryanodine receptor (RyR)/Ca^{2+} release channel of the SR. Unlike cardiac muscle EC coupling, which requires a small amount of extracellular Ca^{2+} to cross the T-tubule, skeletal muscle EC coupling does not require Ca^{2+} movement through the surface membrane for activation of Ca^{2+} release (Armstrong et al., 1972; Spiecker and Luttgau, 1979). Instead, a direct communication between the DHPR and RyR has been proposed to mediate signal transduction (Rios et al., 1991; Rios and Pizarro, 1991). After calcium is released from the SR, the Ca^{2+} - Mg^{2+}-ATPase (Ca^{2+} pump), a 110 kDa protein of the SR membrane, re-accumulates Ca^{2+} into the lumen of the SR. Energy for driving this pump is provided by the hydrolysis of ATP. For each mole of ATP hydrolyzed, 2 moles of Ca^{2+} are pumped into the SR. This results in a decrease of the cytoplasmic free Ca^{2+} concentration and leads to muscle relaxation.

2.2.2 *Sarcoplasmic Reticulum and Calcium Release Channel*

The sarcoplasmic reticulum, as its name suggests, is a membrane system similar to the endoplasmic reticulum (ER) of nonmuscle cells. Unlike the ER, in which

membrane bound proteins and lipids are synthesized, the SR is a highly specialized network for accumulating, storing, and releasing calcium ions in skeletal and cardiac muscle.

The SR can be functionally divided into two components, the longitudinal SR (LSR) and the terminal cisternae (TC) (Fig.5). The LSR is a network of tubules that stretches along the length of each sarcomere (Peachey, 1965), and contains approximately 90% of the Ca^{2+}-Mg^{2+}-ATPases. These proteins continually pump calcium from the sarcoplasm into the lumen of SR. The calcium pump from mammalian muscle tissue is a single polypeptide chain with a known amino acid sequence. A three-dimensional structure has been proposed for this protein that attempts to describe the mechanism by which Ca^{2+} is pumped across the SR membrane (MacLennan and Green 1970) (Fig.6).

The terminal cisternae is found adjacent to the T-tubule, giving rise to a structure called a triad. In electron micrographs a triad appears as three circles in a row. The central circle is the T-tubule membrane, while the circles on each side are the membranes of the terminal cisternae. There is a gap between the TC and the T- tubules

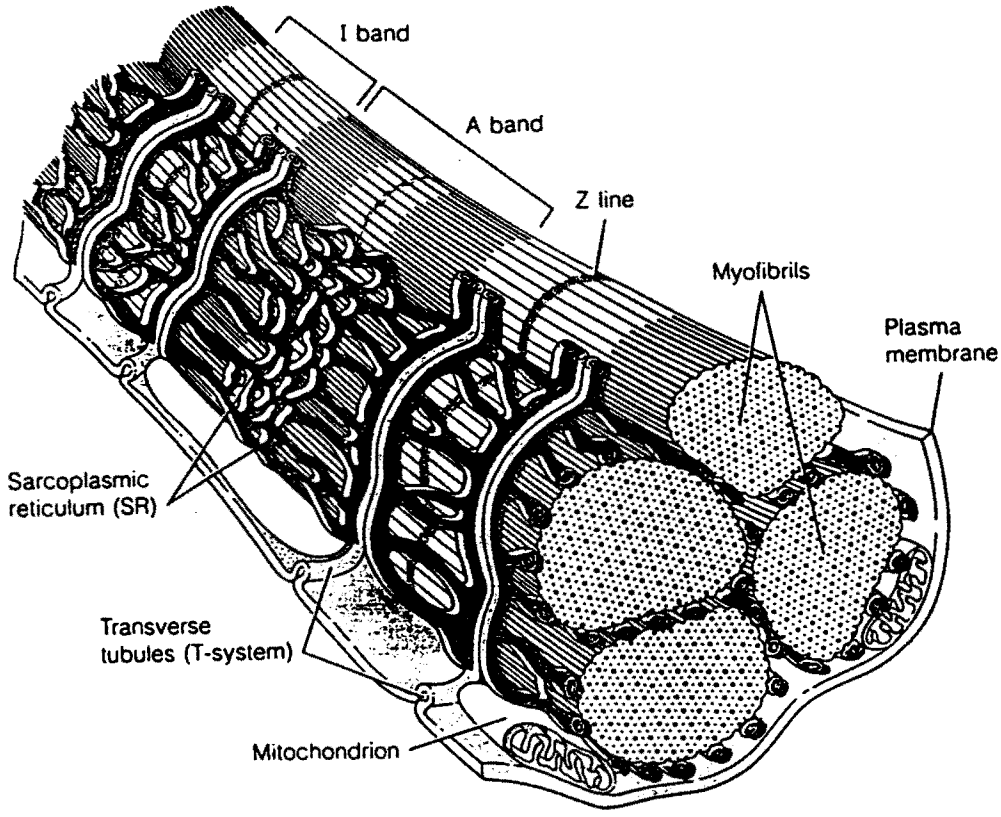

Figure 5. The sarcoplasmic reticulum and the transverse tubule system of striated muscle cells. The sarcoplasmic reticulum (SR) is an extensive network of specialized ER that accumulates calcium and releases it on signal. The transverse tubules of the T-system are invaginations in the plasma membrane that relay the action potential from the plasma membrane to the interior of the cell. (From Voet and Veot).

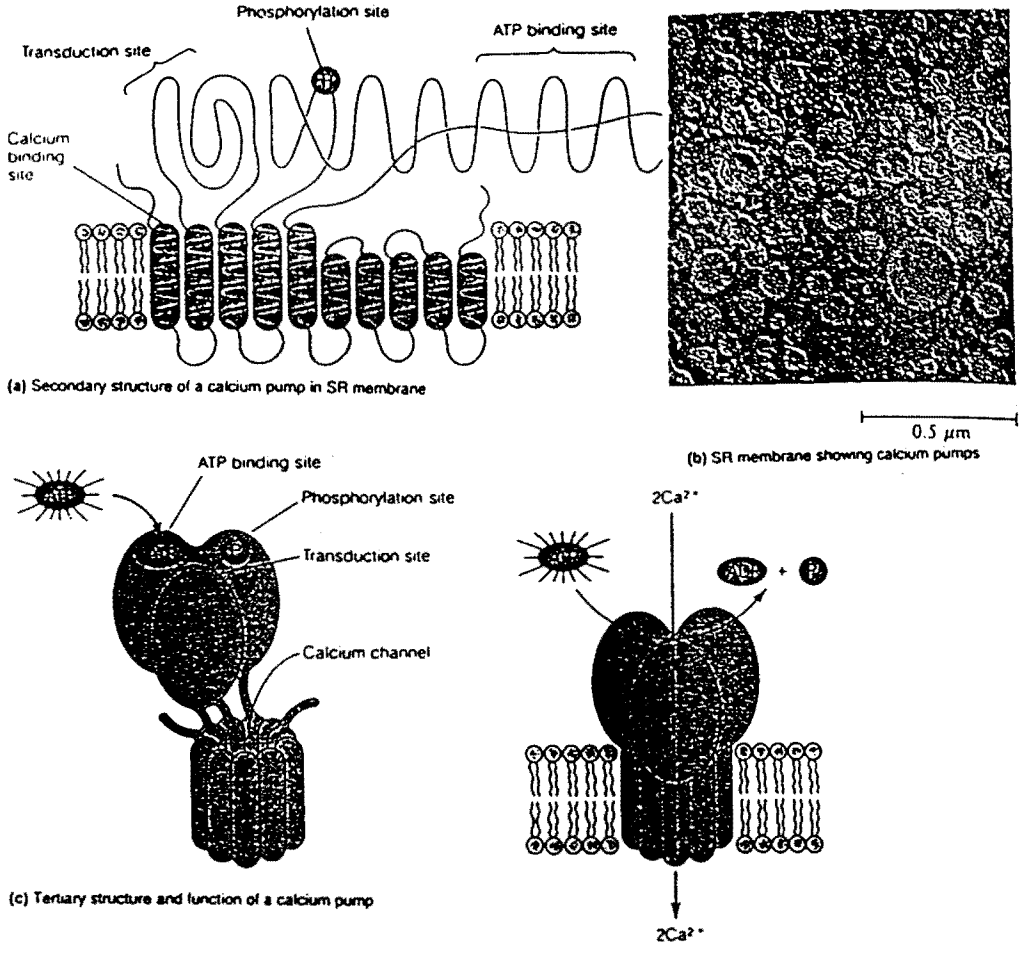

Figure 6. Structure of the Calcium Pump Protein. The calcium pump protein is a single polypeptide chain containing 1001 amino acids. (a) A schematic of the partially unfolded chain indicates its main features. Ten α helices are embedded in the lipid bilayer, and a cluster of helices to form a transmembrane calcium channel. (b) The pump enzyme, the Ca^{2+}-Mg^{2+}-ATPase, can be seen as small particles in the membranes of SR visualized by the freeze-fracture technique (TEM). (c) The head group of the calcium pump has three significant features, including an ATP-binding site, a phosphorylation site, and a transduction site, where the energy from ATP hydrolysis is utilized to pomp Ca^{2+} across the SR membrane. When calcium is present, the ATPase activity is activated, and two calcium ions are transported inward for every ATP hydrolyzed. (From Voet and Voet).

of approximately 120-170 angstroms (Martonosi, 1984). The junctional-foot-protein (JFP), a dense foot-like structure mainly localized in the terminal cisternae region of the SR, connects the T-tubule to the TC. This JFP has been identified as the Ca^{2+} release channel protein (CRC), or ryanodine receptor (RyR). It has a molecular weight of about 565 kDa for each subunit (Takekura et al., 1989), and homotetramers are spaced about 20 nm apart on the membrane of the SR (Lai et al., 1988). The foot structure is associated with the DHPR, the voltage sensor protein, at the terminal area of the T-tubule.

The RyR binds the plant alkaloid ryanodine with a high affinity when the channel is in an open state. The channel associates with adjacent proteins to form a functional protein complex to modulate Ca^{2+} transport into the cytoplasm of the muscle cell, following sarcolemmal excitation. The four identical subunits of this channel (Wagenecht, 1989) span the gap between the terminal cisternae and the transverse tubule membrane system and provide functional coupling to the voltage sensors during EC coupling. The dimensions of the RyR have been estimated to be 29nm × 29nm ×12nm for the cytoplasmic part (Radermacher et al., 1994). Based on the sequence analysis, this high molecular weight protein has four transmembrane regions. Further studies (Wagenecht et al., 1989; Radermacher et al., 1995; Orlova et al., 1996) have provided a picture of the CRC in the open and closed states (Fig.7-9). In its open state,

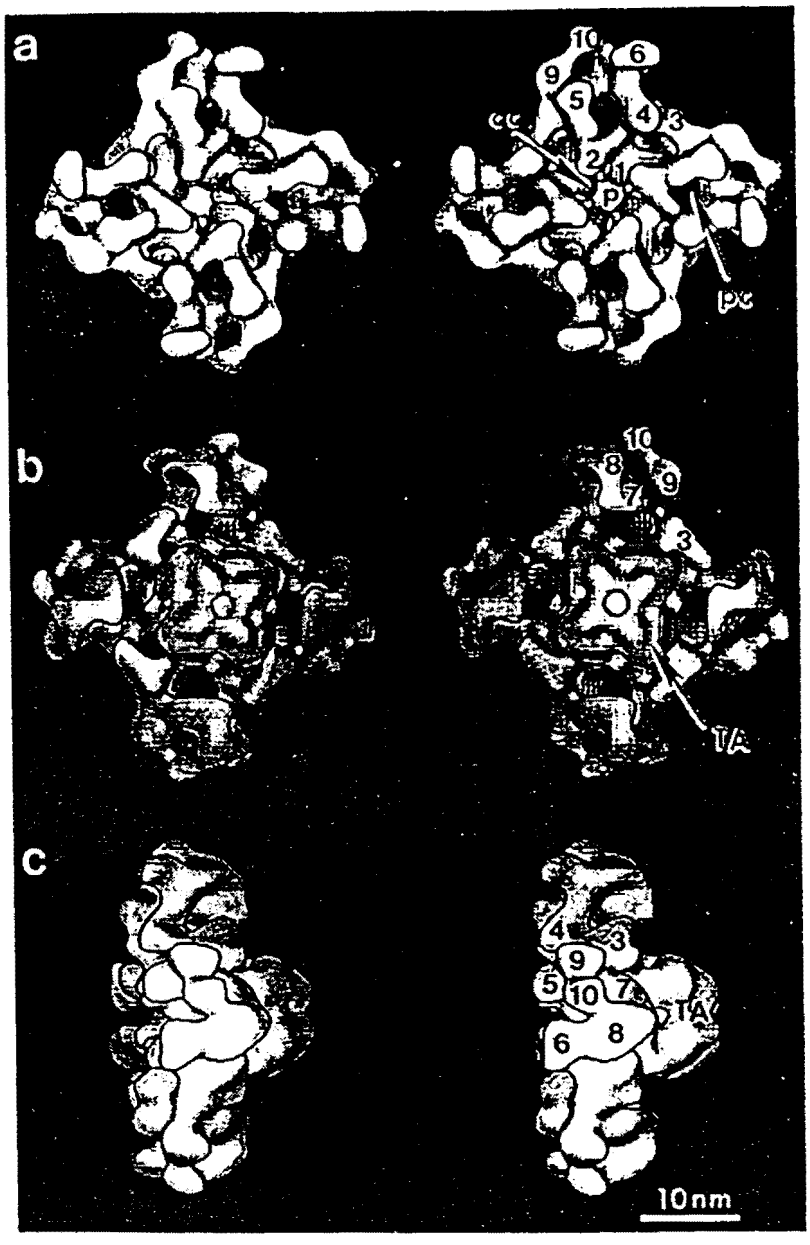

Figure 7. The three-dimensional reconstruction (stereo pairs) of the ryanodine receptor. (a) Surface representation of the cytoplasmic (front) face of the receptor. (b) Surface representation of the transmembrane (back) region of the receptor. (c) Side view of the receptor with the cytoplasmec assembly on the left and the transmembrane domain on the right. The numbers represent putative structural domains. Reproduced from Radermacher et al., 1995.

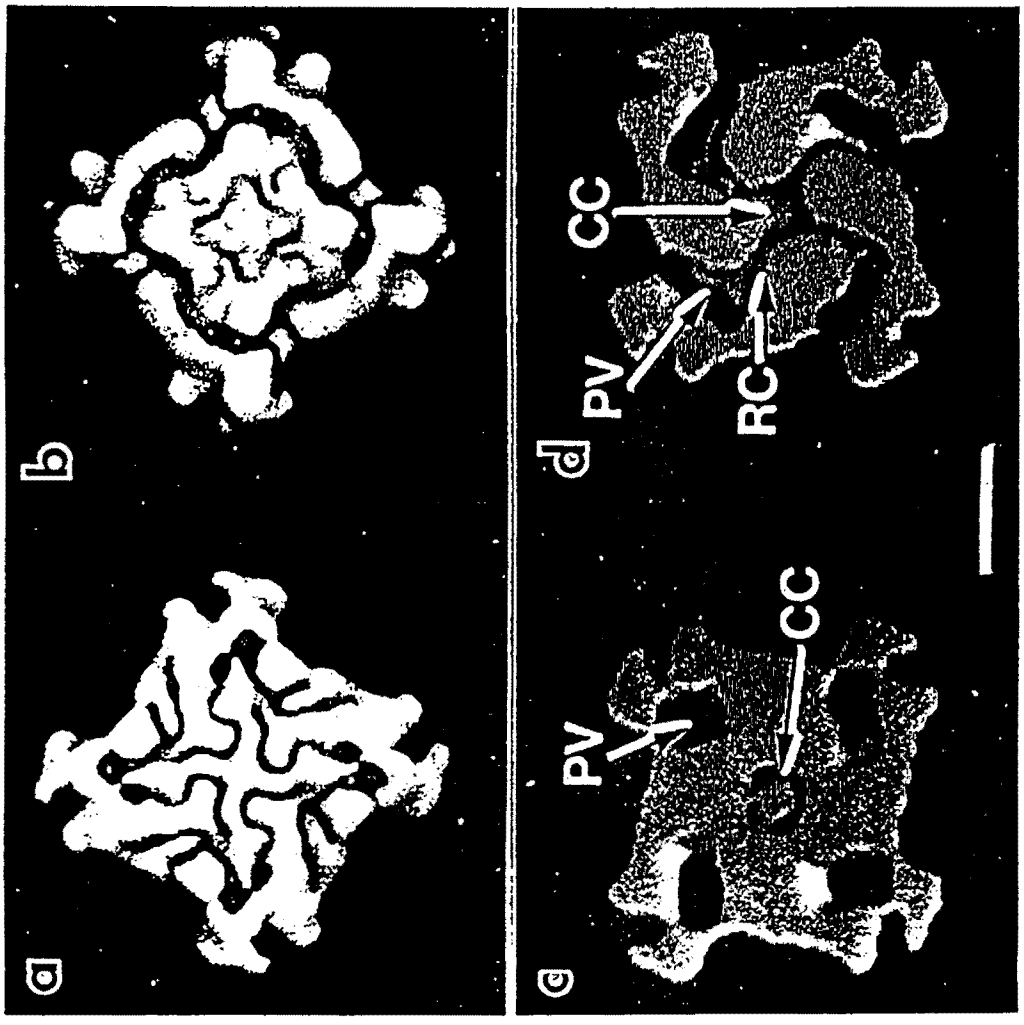

Figure 8. The three-dimensional structure of the ryanodine receptor. Reconstruction obtained from negatively stained specimens. Labeled are the central cavity (CC), the radial canal (RC), and peripheral vestibules (PV). (a, b) Top and bottom faces; (c, d) reconstruction spliced open to reveal internal structure. Reproduced from Wagenecht et al., 1989.

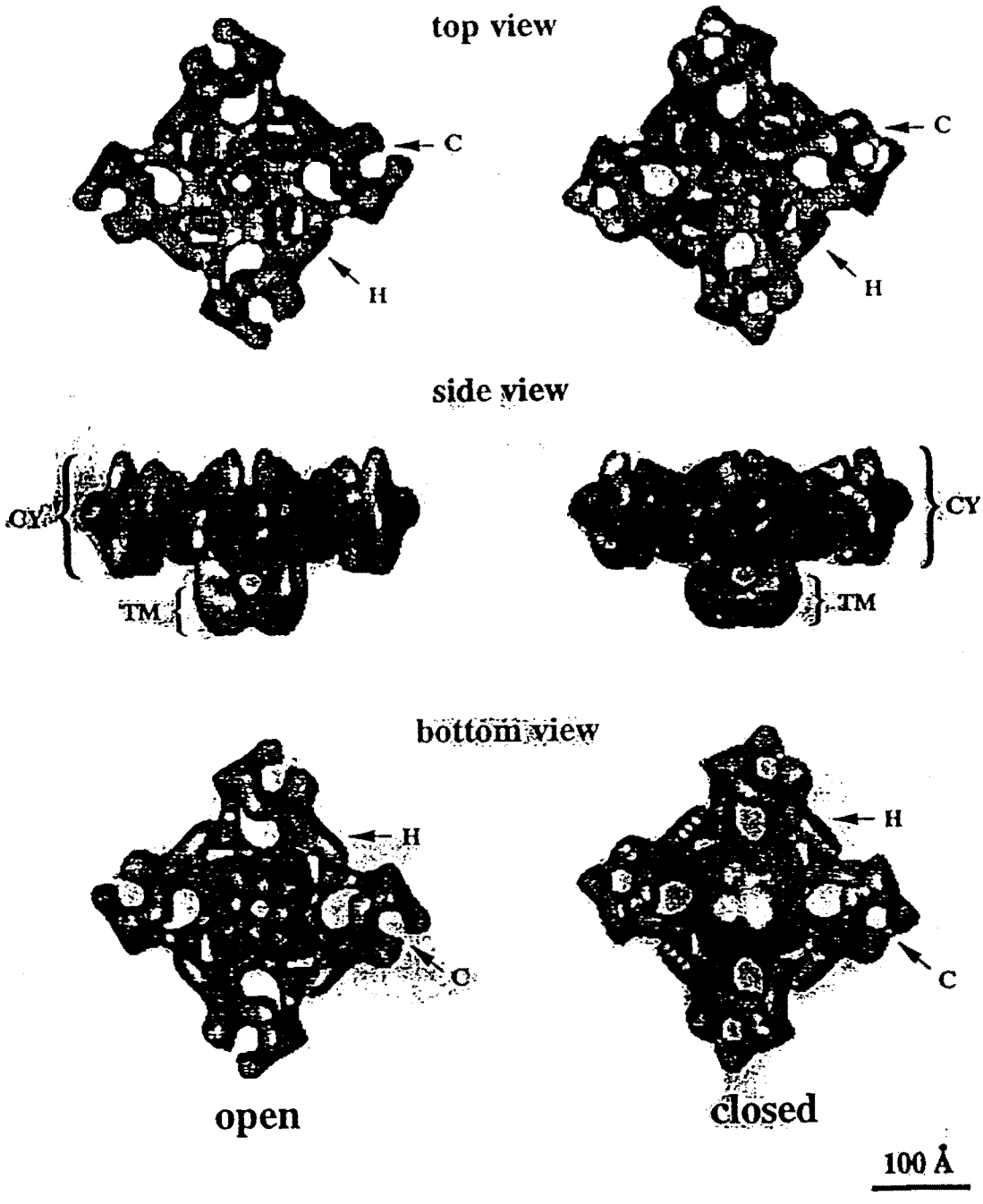

Figure 9. The open and closed states of the ryanodine receptor. Labeled are the clamp-shaped domain (C), the handle (H) which connects the clamp-shaped domain to the central part of the cytoplasmic side (CY) of the tetramer, and the putative transmembrane (TM) domain. Reproduced from Orlova et al., 1996.

the CRC appears to have a central pore, approximately 2nm wide and 2nm deep, and four radial channels. This protein is cation selective, with a high single channel conductance. It has recently been suggested that the RyR forms disulfide-linked dimers during channel activation (Aghdasi et al., 1997).

The lumen of the TC is also filled with dense granular bodies which are not present in the LSR. The dense bodies have been identified as the low affinity Ca^{2+} binding protein, calsequestrin (MaClennan & Wong, 1971). Because of the high protein density of calsequestrin, TC vesicles (heavy SR vesicles) can be separated from LSR vesicles (light SR vesicles) by means of density-gradient centrifugation (Meissner, 1975).

A large amount of evidence suggests that the CRC functionally interacts with a number of junctional proteins during calcium release from SR. These proteins include triadin, FKBP12, DHPR, and calsequestrin (Fig.10). Triadin is a 95 kDa glycoprotein isolated from heavy SR (Caswell et al., 1991; Guo and Campbell 1995). This protein appears to cross-link to the RyR to form a high molecular weight complex. It also binds to the DHPR with a high affinity, and may participate in E-C coupling. However, Flucher et al. (Flucher et al., 1993) have provided evidence that calsequestrin is involved in calcium storage and Ca^{2+} release system from SR during E-C coupling. They found that dysgenic myotubes with a deficiency in the alpha 1 subunit of the DHPR show reduced expression and clustering of the RyR and mature cross-striated distributions. On the other hand, calcium waves (which is believed to be Ca^{2+} -induced-

Ca^{2+} -release) were also frequently observed in dysgenic myotubes and their properties were unchanged compared to normal myotubes, but, both proteins are still capable of forming clusters. However, depolarization-induced calcium release is absent. Thus, characteristic calcium release properties of the RyR do not require interactions with the DHPR. These results strongly suggested that, a) the molecular organization of the RyR and triadin in the terminal cisternae of the SR, as well as its association with the T-tubules, are independent of interactions with the DHPR; and b) the function of the calcium storage and release system are independent during E-C coupling (Flucher et al., 1993, Carl et al., 1995).

FKBP12, a ubiquitous 12 kDa protein tightly bound to the skeletal muscle RyR in four positions, appears to be directly adjacent to the "clamp-like" domain described by Orlova et al. (1996). It is at least 10nm away from the membrane spanning domain ,with one FKBP12 per RyR monomer (Jayaraman et al., 1992; Timerman et al., 1993). The single FKBP12-depleted RyR channel appears to exist in three substate activity levels of ~0.25, ~0.5, and ~0.75 of the normal maximum conductance (Ahern et al., 1997). The DHPR is an L-type Ca^{2+} channel found in the T-tubule. It has a conductance of ~ 25pS and is activated by a large positive membrane potential. It serves as the voltage sensor during EC coupling. Calsequestrin, a 60 kDa lumenal protein, appears to be tightly associated with the junctional protein triadin (Collins et al., 1990; Ikemoto et al., 1989), and has >40 Ca^{2+}-binding sites. Its major role is in the storage of Ca^{2+} in the SR. However, studies of its conformational

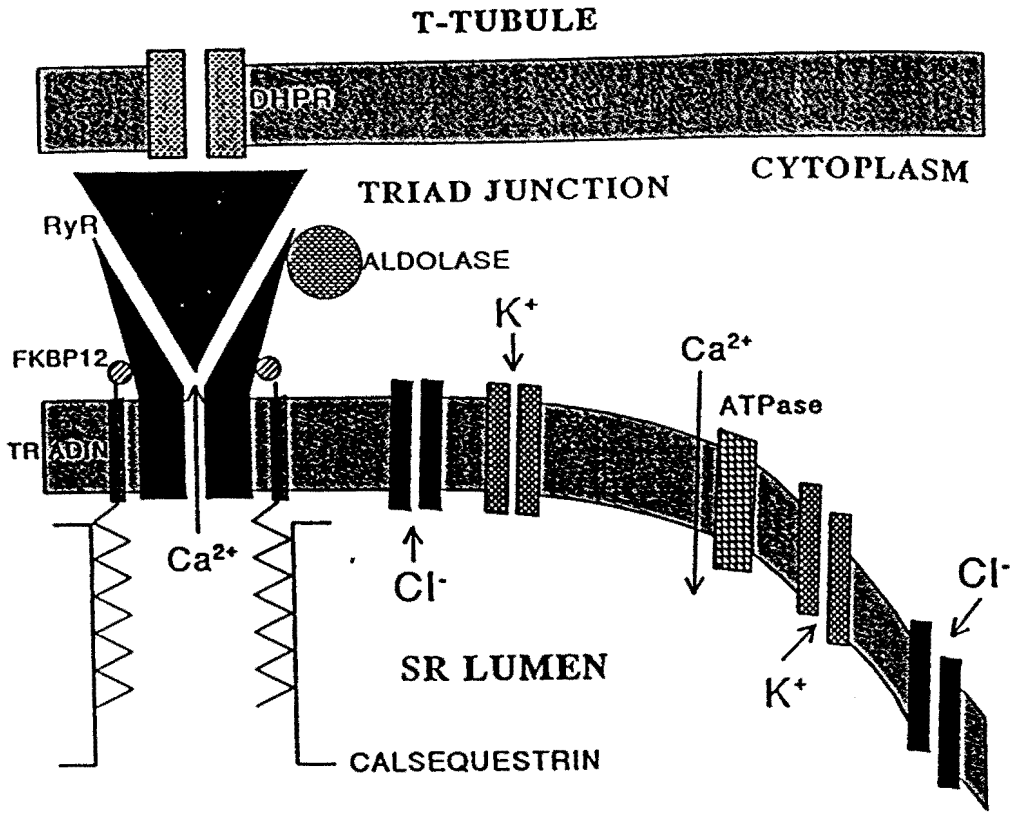

Figure 10 A schematic illustration of the location of the junctional proteins and ion channels in the SR and T-tubule membranes (Dulhunty et al., 1996). The DHPR is the main protein in the T-tubule membrane associated with EC coupling. RyRs in the SR membrane are closely associated with DHPRs. The large cytoplasmic domain of the RyR is located within the junctional gap between the T-tubule and the SR. Two proteins, aldolase and the FK-506 binding protein (FKBP12), are closely associated with the cytoplasmic domain of the RyR. Triadin which is also associated with the RyR has a single transmembrane segment and a lumenal domain which may interact with the Ca^{2+} binding protein calsequestrin. (Dulhunty et al. 1996)

changes during the Ca^{2+} release process suggest a possible role in the regulation of release.

2.2.3 *The Redox Model of Calcium Release Channel Complex*

A number of redox reagents modulate Ca^{2+} release from the SR through the Ca^{2+} release channel RyR. Reagents that stimulate Ca^{2+} release from the sarcoplasmic reticulum include heavy metals such as Hg^{2+}, Ag^{+}, Cu^{2+}, Cd^{2+}, and Zn^{2+} (Abramson et al., 1983; Salama et al., 1984), anthraquinones (Abramson et al., 1988), reactive disulfides (Zaidi et al., 1986), naphthoquinones (Liu et al., 1994; Liu et al., 1995), rose bengal (Stuart et al., 1992; Xiong et al., 1992), and oxidized glutathione (GSSG) (Zable et al., 1997). In contrast, reducing agents, such as DTT and reduced glutathione (GSH), inhibit the activity of the Ca^{2+} release channel. This can be observed either at the single channel level or at the ryanodine binding level. In 1994, Pessah and his research group, using a fluorogenic coumaryl maleimide (CPM), described the presence of a discrete class of highly reactive thiols associated with the CRC of the SR and other junctionally related proteins (Liu et al., 1995). They also described a disulfide-linked high molecular weight complex (HMWC), comprised of the CRC, triadin, and several other junctional proteins. Takeshima and his co-workers have provided further evidence that there are about 100 cysteines on each subunit of the Ca^{2+} release channel tetramer (Takeshima et al., 1989), and there are only two known sulfhydryls on triadin (Knudson. et al., 1993). In addition, Quinn and Ehrlich have

recently observed a reduction of the single channel conductance of the CRC, when the cysteines on the channel are modified by methanethiosulfonate compounds. They also suggest that there are reactive sulfhydryls in the ion conducting pathway (Quinn et al., 1996) that modify normal function of the receptors.

These studies finally lead to a model for the redox modulation of the CRC that involves several sulfhydryl groups, existing in close proximity and able to form mixed disulfides, to regulate the opening and closing of the channel. Oxidation of the key

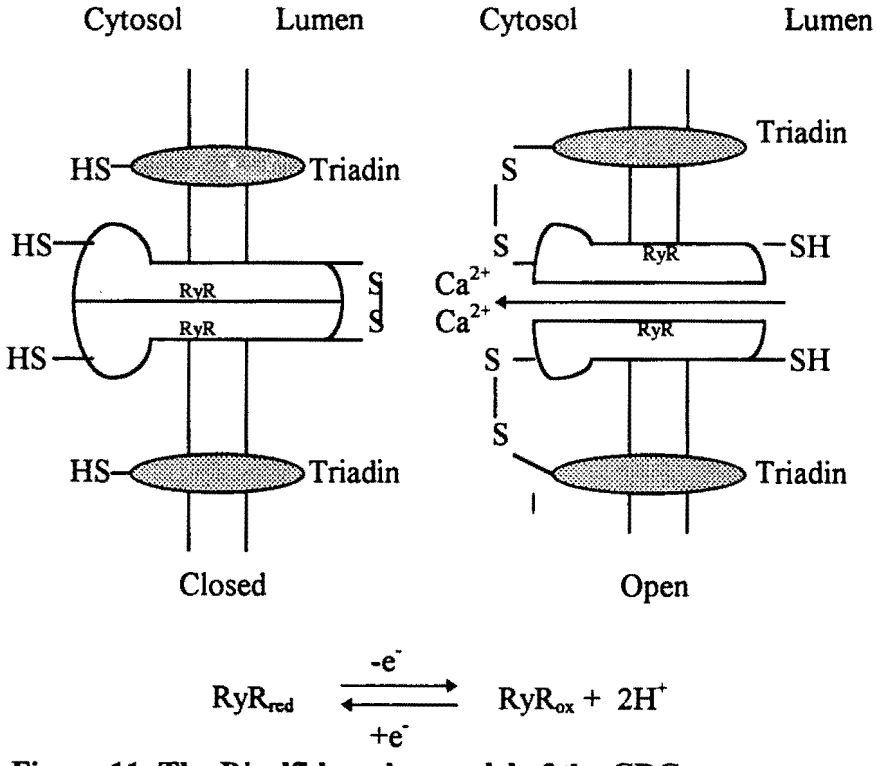

Figure 11. The Disulfide redox model of the CRC.

thiols in the active sites results in the formation of a mixed disulfide-linked multiprotein complex and the opening of the CRC. Reduction of these disulfides results in the dissociation of this complex and the closure of the CRC (Fig. 11).

2.2.4 *The IP_3 Receptor, a similar intracellular Ca^{2+} channel*

There is considerable evidence that an intracellular Ca^{2+} release channel, the IP_3 receptor, is similar to the RyR in its general organization (Pozzan et al., 1994). Inositol 1,4,5-triphosphate (IP_3) is an intracellular messenger which has been shown to trigger Ca^{2+} release from the endoplasmic reticulum of several tissues. It has been reported that IP_3 induces Ca^{2+} release in cardiac, skeletal and smooth muscle (Suematsu et al., 1984; Hasegawa et al., 1989). In contrast, IP_3 does not modify ryanodine binding to either type of muscle. Moreover, it has been reported that phosphatidylinositol 4,5-bisphosphate (PIP_2) elicits a 2-12 fold increase in the open probability of the reconstituted single channel (Chu and Stefani, 1991). A model was proposed in which depolarization of the T-tubule membrane stimulates phospholipase C activity that hydrolyzes PIP_2 to IP_3. IP_3 then diffuses to an IP_3 receptor, activating the receptor to cause calcium release. The IP_3 receptor is a 300 kDa monomeric protein, and is similar in shape to the RyR. This protein is widely expressed in the ER of many cell types, but its role in striate muscles still remain controversial. It is believed that about 8% of the IP_3 receptor is attached to the cytoskeletal protein ankyrin.

This attachment could be important in the regulation of the function and the co-localization of the receptor (Bourguignon et al., 1993).

3 THE MODULATORS OF THE CALCIUM RELEASE CHANNEL RyR

3.1 Introduction

A number of chemical compounds have been found that modulate the Ca^{2+} release channel activity of the sarcoplasmic reticulum. These compounds either activate or inhibit the CRC by influencing Ca^{2+} efflux or ryanodine binding to the channel. With the use of these compounds, it is possible to investigate the nature of the CRC, to determine how endogenous factors regulate the activity of this channel.

Table 1: Modulators of the SR Ca^{2+} Release Channel (Modified from Coronado et al., 1994)

Stimulators	Effective Concentration	Inhibitors	Effective Concentration
Ca^{2+}	0.1-100μM	Ca^{2+}	>1mM
Adenine Nucleotides	1-5mM	Mg^{2+}	0.5-5mM
Caffeine	>0.5mM	Ruthenium Red	0.01-20μM
Ryanodine	5-40nM	Ryanodine	>10μM
Ag^{+}	5-50μM	Calmodulin	0.2μM
Cu^{2+}/cysteine	2/10μM	Lactate	10-20mM
Reactive disulfides	1-20μM	Procaine	1-20mM
Doxorubicin	5-50μM	Tetracaine	0.1-2mM
Rose bengal	1-2nM	CPM	10-100nM
Porphyrins	1-60μM	Neomycin	0.01-20μM
GSSG	0.5-2mM	GSH	1-5mM

3.2 Activators of the Calcium Channel

Ca^{2+} has a biphasic role in regulation of the Ca^{2+} release channel. Low Ca^{2+} concentrations (~μM) stimulate the Ca^{2+} release channel of the SR, while high Ca^{2+} concentrations (>1mM) inhibit the channel. The interaction between cytosolic Ca^{2+} and the CRC is now well understood. It is believed that there are two distinct sites for Ca^{2+} binding to the RyR, a high affinity binding site which is responsible for channel activation, and a low affinity site for the channel inhibition (Smith et al., 1986). There is a parallel Ca^{2+} release mechanism in the SR, termed the Ca^{2+}-induce-Ca^{2+}-release, which is believed to be independent of the E-C coupling in the skeletal muscle (Flucher et al., 1993), but is not in the cardiac muscle (Fabiat 1983).

Caffeine is one of the better known muscle stimulators. It is known to induce muscle contraction, and to activate myofibril contraction independent of T-Tubule depolarization (Sandow and Brust, 1996). Caffeine is shown to stimulate Ca^{2+} efflux from SR vesicles, and to enhance ryanodine binding by dramatically increasing the affinity of the Ca^{2+} activator site for Ca^{2+} (Pessah et al., 1986).

Adenine nucleotides are also known as endogenous CRC stimulators. They increase the gating efficiency and the life time of the open state of the Ca^{2+} release channel. Unlike the case of the Ca^{2+} pump, ATP is not hydrolyzed when it interacts with the calcium release channel.

Quinones are known to undergo redox cycling reactions in a number of biological systems. They can be reduced by a single electron to a semiquinone free radical form, or by two electrons to a hydroquinone form. They also have been suggested to form electron-transfer complex (Smith 1986) with electron donors such GSH or DTT and partially gains a electron from them. In the sarcoplasmic reticulum, naphthoquinones, such as menadione (Vitamin K_3) and 1,4-naphthoquinone have been shown to induce calcium efflux from the SR vesicles. Pessah's research group has shown that 1,4-naphthoquinone selectively oxidizes hyperreactive sulfhydryls on the RyR and opens the Ca^{2+} release channel. It also oxidizes sulfhydryls on RyR1 and triadin to generate a cross-linked product. This cross-linked high molecular weight complex (HMWC) is reduced by β-mercaptoethanol or DTT into its component RyR1 and traidin protomers (Liu et al., 1994; Liu et al., 1995). The anthraquinone doxorubicin, a potent anticancer reagent, greatly enhances ryanodine binding to the RyR and stimulates Ca^{2+} efflux from actively loaded SR vesicles (Abramson et al., 1988).

3.3 Inhibitors of the Ca^{2+} Release Channel

Mg^{2+} has long been known to inhibit contraction of muscle fibers (Ford and Podolsky, 1970; Endo et al., 1970), to inhibit Ca^{2+} release from isolated SR vesicles (Fairhurst et al., 1970), and to inhibit single channel activity in lipid bilayers (Smith et al., 1986). Compared to ruthenium red, Mg^{2+} is less effective as an inhibitor, but is

more physiologically relevant, since Mg^{2+} occurs in the muscle cells in concentrations of 0.6-1.0 mM. Mg^{2+} is believed to inhibit Ca^{2+} release by decreasing the apparent affinity of the activator site for Ca^{2+} (Pessah et al., 1987).

One of the most effective inhibitors of the Ca^{2+} release process is ruthenium red (RR) (Moore, 1977; Ohnishi, 1979; Meissner et al., 1986; Salama and Abramson, 1984; Trimm et al., 1986). The mechanism by which RR inhibits the CRC is still unclear. Recent results indicate that the RR binding sites may be co-localized with the Ca^{2+} binding sites (Chen et al., 1994). Unlike Mg^{2+}, RR inhibition of CRC is irreversible.

Reducing agents, such as dithiothreitol (DTT) and glutathione (GSH), also inhibit the CRC (Zable et al., 1997).

CHAPTER 2

GENERAL METHODS

1. PREPARATION OF SARCOPLASMIC RETICULUM

All experiments were performed with SR vesicles isolated from white (fast) muscles of the back and legs of 2 to 3 kg New Zealand White male rabbit according to the methods of MacLennan et al., (1970). Rabbits were injected with 3 ml sodium pentobarbital and then bled by cutting the jugular vein. The muscles were quickly removed, and the fat and connective tissues trimmed. The muscles were minced into Buffer A (120 mM NaCl, 10 mM imidazole, 100 μM dithiothreitol (DTT), 200 μM leupeptin, pH 7.4), and put on ice. The minced muscle was then homogenized in a Waring Blender until the homogenate was smooth (alternating low and high speed for 15 seconds/45 seconds, 1 minute between cycles, 4 cycles). The resulting homogenate

was centrifuged at 1,600×g (3,100 rpm in a large Sorvall GSA rotor) for 10 minutes, and the remaining muscle debris and tissue was discarded. The supernatant fraction was then filtered through four layers of cheesecloth and adjusted to pH 7.4 with dry imidazole. The supernatant was centrifuged again for 15 minutes at 10,000×g (8,000 rpm in the large Sorvall GSA rotor). The resulting supernatant was again strained through four layers of cheesecloth, and the brown mitochondrial pellet was discarded. The supernatant was then centrifuged at 44,000×g (19,000 rpm in the Ti19 rotor) for 70 minutes. The clear supernatant was carefully discarded and the protein in the pellet, above the brown mitochondrial ring, was re-suspended in Buffer A (without DTT or leupeptin) to a final concentration of approximately 10 mg/ml with a Wheaton glass homogenizer. This suspension was then centrifuged at 7,500×g (11,000 rpm in the Ti60 rotor) for 10 minutes. The supernatant was carefully pipetted off and kept without disturbing the floculant myosin pellet. This solution was again centrifuged at 78,000×g (35,000 rpm in the Beckman Ti60 rotor) for 30 minutes. The pellet containing the SR vesicles was suspended into Buffer B (100 mM KCl, 20 mM Hepes, pH 7.0) at a final concentration of about 25 mg/ml (~15-20 ml final volume). The SR was stored in small tubes in liquid nitrogen.

2 DETERMINATION OF PROTEIN CONCENTRATION

Protein concentrations of the SR preparations were determined by the method of Kalckar (1947). The absorbance peak at 280 nm is primarily due to tyrosine and tryptophan residues. The absorbance peak at 230 nm is due to the peptide bonds in the proteins. Protein concentration was calculated according to the following equations:

$$[SR]_{mg/ml}=(1.45*A_{280}-0.74*A_{260}) \quad .....(1)$$

$$[SR]_{mg/ml}=(0.185*A_{230}-0.075*A_{260}) \quad .....(2)$$

where A_{280}, A_{260}, A_{230} are the absorbances at each wavelength. The terms containing A_{260} in the above equations are correction factors to eliminate the possibility of contamination by nucleic acids, which absorb strongly at 260 nm. Measurements were made in duplicate at several different dilution of the SR.

The final protein concentration was calculated as a mean standard deviation.

3 CHEMICALS

All quinones and reagents not specifically listed below were purchased from Sigma Chemical Co. Ryanodine and ^{3}H-ryanonodine were purchased from Du Pont with a specific activity of 75-80 Ciu/mmol.

1,4-naphthoquinone (1,4NQ) and 1,2-naphthoquinone (1,2NQ) stock solutions were prepared in DMSO. Mg-ATP was stored in liquid N_2. A23187, creatine

phosphate (CP), creatine phosphokinase (CPK), GSH, and both labeled and unlabeled ryanodine were stored at -4^{0}C. $CaCl_2$, and ethyleneglycol-bis-(β-aminoethyl ether) N,N,N',N'-tetraacetic acid (EGTA) were stored at room temperature.

4. Ca^{2+} EFFLUX STUDIES

Ca^{2+} efflux from actively loaded SR vesicles was examined as a function of quinone concentration. Ca^{2+} uptake and release from SR vesicles were measured using a dual wavelength spectrophotometer (custom manufactured by the University of Pennsylvania machine shop) through the differential absorption changes of antipyralazo III (APIII), a metallochromic indicator of extravesicular free Ca^{2+} (Chance et al., 1975). Differential absorption was measured at 720-790 nm. Reagents such as CP, CPK, ATP, GSH, and RR, as well as DTT, at the concentrations used in this study produced negligible changes in the absorbance of APIII, and did not interfere with measurements of the free Ca^{2+} concentration in the medium. Unless otherwise stated, measurements of Ca^{2+} transport were carried out in 1.5 ml of assay medium containing 0.2 mg/ml SR protein in a buffer of 200 μM APIII, 100 mM KCl, 20 mM Hepes, pH 7.0, at room temperature. The cuvette was placed in the spectrophotometer and an aliquot of Ca^{2+} (20 μM) was manually added to the media to calibrate the APIII signal. Active Ca^{2+} uptake was initiated by adding an ATP-regenerating system containing 5-10 units CP and ~1μg/ml CPK followed by 1mM Mg-ATP. Upon completion of Ca^{2+} uptake, several aliquots of Ca^{2+} were added until the SR vesicles were maximally

loaded. Release was initiated by the addition of an effluxing agent (i.e. 1,4NQ). The maximal slope of the time-dependent absorbance change was related to the maximum rate of Ca^{2+} release in nmol/mg/sec. The total amount of Ca^{2+} in the lumen of the vesicles was determined by addition of 2 μg/ml of the Ca^{2+} ionophore A23187. In several experiments, DTT, GSH or RR were added to the reaction mixture to test for the inhibition or reversal of Ca^{2+} release.

5 [^{3}H] -RYANODINE BINDING ASSAYS

5.1 Introduction

Ryanodine is a neutral alkaloid isolated from the plant Ryania speciosa Vahl. Ryanodine acts as a natural insecticide for the plant by inducing an irreversible muscle contraction in the insect. The extended rise in cellular Ca^{2+} levels leads to cell death. Ryanodine interacts with the calcium release channel and locks it in the open state. As a result of this, the intracellular Ca^{2+} concentration rises and the muscle goes into rigor. Research shows this compound not only activates the RyR in skeletal muscle to induce an irreversible contraction, but it also decreases contractile force in cardiac muscle .

The use of ryanodine, labeled and unlabelled, has significantly enhanced our understanding of the function of the SR Ca^{2+} release channel. Tritium labeled ryanodine ([^{3}H]ryanodine), is extensively used in ligand binding assays. It has been shown that ryanodine remains tightly bound with a nanomolar affinity to a single class of proteins near the junctional region of the SR (Pessah et al., 1985; Pessah et al., 1986). With a

few exceptions, such as silver, compounds that stimulate Ca^{2+} release via the opening of the Ca^{2+} channel also stimulate the binding of ryanodine to its receptor, whereas the compounds that inhibit Ca^{2+} release by closing the Ca^{2+} channel also inhibit ryanodine binding. Like Ca^{2+}, ryanodine induces a biphasic response upon binding to its receptor. At 5-40 nM, ryanodine stimulates channel activity, while at >10 μM it inhibits transport across SR and single channel activity. It is believed that any chemical compound which changes the characteristics of ryanodine binding interacts with the Ca^{2+} release channel. There are four binding sites on the RyR corresponding to the four monomers of this channel.

5.2 Equilibrium Ryanodine Binding

5.2.1 *Conventional Ryanodine Binding*

[^{3}H]-ryanodine equilibrium binding assays were carried out according to the method described by Pessah et al., 1987. SR vesicles (0.5 mg/ml) were incubated at 37^{0}C for 3 hours in a medium containing 1nM [^{3}H] ryanodine, 14 nM ryanodine, 250 mM KCl, 15 mM NaCl, 25 mM Hepes and 10 μM $CaCl_2$, pH 7.1(KOH). Depending on the experimental conditions, various channel modulators were added in the medium. After 3 hours equilibrium binding was achieved and the reaction was quenched by rapid filtration through a Whatman GF/B glass fiber filter, using a cell harvester (Brandel, Gaithersburg, PA). Filters were then washed three times with ~5 ml of buffer containing 250 mM KCl, 15 mM NaCl, and 20 mM Tris, at pH 7.1 (HCl). The filters

were then placed into scintillation vials, incubated with 3ml of scintillation fluid (Beckman, ReadySafe or ICN, CytoScint) and were shaken overnight. The radioactivity was counted by a scintillation counter with an efficiency of approximately 55 %. Non-specific binding was measured in the presence of a 200-fold excess of unlabeled ryanodine. Total specific activity was determined by adding 10 µl of the experimental medium in 3ml scintillation fluid and counting the sample.

5.2.2 *Scatchard Analysis of High Affinity Ryanodine Binding*

By measuring high affinity ryanodine binding versus the concentration of ryanodine it is possible to determine the equilibrium binding constant, K_d, and the maximal number of binding sites, B_{max}. In these experiments, 0.5 mg/ml SR protein was incubated at 37^0C for 3 hours with various concentrations of [^{3}H] ryanodine (1 - 64). Scatchard analysis was carried out using a one-site model. In this analysis, the ratio of bound to free ryanodine (B/F) was plotted vs. bound ryanodine (B).

$$B/F = (B_{max} - B) / K_d \qquad (3)$$

where B_{max} is the maximum number of binding sites, and K_d is the concentration of ryanodine at which half of the high affinity binding sites are occupied. The slope of the Scatchord plot is $-1/K_d$, and the x-intercept is B_{max}. The resulting Scatchard plot with a single class of binding sites yielded excellent fits to a straight line.

5.2.3 *Hill Analysis of Binding Data*

A Hill analysis and formula was used to analyze the cooperativity of ligand interactions with a receptor. [^{3}H] ryanodine binding data were fit to:

$$B = (B_{max} [A]^n)/(K_d+[A]^n). \quad (4)$$

Taking the natural logarithm of both side of the equation yields:

$$\ln(B/(B_{max}-B))= n\ln([A]) -\ln(K_d) \quad (5)$$

where B is the amount of ryanodine bound (pmol/mg), [A] is the concentration of a modulator, B_{max} is the maximal amount of ryanodine bound in the presence of the modulator, K_d is the apparent affinity of the binding site for A, and the apparent Hill constant, *n*, is a measure of the degree of cooperativity between the ryanodine binding sites. Positive cooperativity is characterized by a Hill constant greater than 1, whereas a value less than 1 indicates negative cooperativity. The data was plotted as $\ln(B/(B_{max}-B))$ vs. ln[A] between 20-80% of B_{max}, and resulted in a straight line. The y-intercept is equal to $-\ln K_d$, whereas the EC_{50}, the concentration of modulators at which 50% saturation occurs, equals $K_d^{1/n}$. If there is no cooperativity (n=1), EC_{50} will be equal to K_d.

5.3 Kinetic Binding Experiments

5.3.1 *Association Ryanodine Binding and Analysis*

Association experiments were carried out to investigate the binding kinetics of various ligands to their receptors. The time course chosen for these experiments was from 2 to 180 minutes. Solution A contained binding buffer (no Ca^{2+}) as described

before with 30 nM ryanodine (2nM [^{3}H] ryanodine, and 28 nM cold ryanodine). Solution B (1mg/ml SR, 20 μM Ca^{2+}, in the conventional binding buffer) was added to solution A, with or without different concentrations of 1,4 naphthoquinone, at each time point. The resulting mixtures, with final concentrations of 0.5 mg/ml SR, 1nM [^{3}H] ryanodine, 14 nM ryanodine, and 10 μM Ca^{2+}, were incubated at 37^{0}C for varying amounts of time. All reactions were quenched by rapid filtration. Non-specific binding was determined from control samples at t=0. The total activity was determined by scintillation counting of 50μl of solution A, without incubation or filtration.

In order to determine the association rate constant, the data was fit to the following equation

$$B(t)=B_{max}\,(1-e^{-Kt}), \qquad (6)$$

Taking the natural logarithm of both side of the equation yields:

$$\ln((B_{max}-B(t))/B_{max}) = -Kt. \qquad (7)$$

A derivative of both sides of equation (6), evaluated at t=0, yields:

$$dB(0)/dt = B_{max}\,K. \qquad (8)$$

where K, the apparent rate constant, is related to the association rate constant k_{+1}, and the dissociation rate constant k_{-1}, by the following equation:

$$K = k_{+1}\,[R] - k_{-1} \qquad (9)$$

The initial rate of ryanodine binding ,dB(0)/dt ,is given by equation (10):

$$dB(0)/dt =[R]\,B_{max}\,k_{+1}. \qquad (10)$$

where [R] is the free ryanodine concentration at t=0.

By plotting $\ln((B_{max}-B)/B_{max})$ versus time t, the apparent rate constant K can be determined. The association rate constant k_{+1} can then be calculated from equation (9) following determination of the dissociation rate constant, k_{-1}.

5.3.2 *Dissociation Ryanodine Binding and Analysis*

To determine the dissociation rate constant k_{-1}, the time dependence of dissociation of the equilibrated [^{3}H] ryanodine-protein complex was measured in the presence and absence of 1,4-naphthoquinone.

For this experiment, solution A, containing 5 mg/ml SR, 5nM ryanodine, 5nM [^{3}H] ryanodine in conventional binding buffer, was incubated at 37^{0}C for 3 hours. The dissociation reaction was initiated by a 100 fold dilution into normal binding buffer, either with or without 50μM 1,4NQ. Samples were then initiated at 37^{0}C. The dissociation reaction was then quenched by removal of 2 ml of the diluted samples to an ice bath. Non-specific binding was obtained by incubating a fraction of solution A with 2mM EGTA at 37^{0}C for 3 hours, followed by a 100 fold dilution into normal binding buffer. This sample was then incubated at 37^{0}C for 30 minutes, before removal to ice. Total activity was obtained from 10 μl samples of solution A immediately prior to the dilution. At 180 minutes, all samples were filtered through a Whatman GF/B filter , and handled in the same manner as in a conventional binding assay.

The dissociation of bound ryanodine can be described by the following equation:

$$B(t) = B(0) \exp(-k_{-1} t) \qquad (11)$$

where k_{-1} is the dissociation rate constant, B(t) is the amount of ryanodine bound at time t, and B(0) is the binding at t = 0. The natural logarithm of both sides of equation (11) yields:

$$\ln(B(t)/B(0)) = -k_{-1} t \qquad (12)$$

The dissociation rate constant k_{-1} is found by plotting the natural logarithm of B(t)/B(0) versus time t.

5.4 Introduction to Quinones

Quinones are diketones derived from aromatic compounds. They are ubiquitous in nature, quinones are found in higher plants, fungi, bacteria, and throughout the animal kingdom. As a good electron receptor, they are centrally involved in many biochemical processes related to electron transport systems, such as photosynthesis, cellular respiration and intracellular Ca^{2+} equilibrium, due to their ability to participate in biological redox reactions.

Quinones can accept electron(s) from electron donors to undergo redox cycling, in which one-electron reduces the quinone to a paramagnetic semiquinone radical. The semiquinone can then autooxidize back to the quinone (Fig.12). In this process oxygen is reduced to yield superoxide (Kappus and Sies, 1981; Powis et al., 1981; Lind et al., 1982; Thor et al., 1982). On the other hand, the two-electron reduction of a quinone

yields a hydroquinone, which tends to be relatively stable and does not readily undergo redox cycling. This is more likely to be a protective pathway than a toxic one.

In the cell, 1,4-naphthoquinones can undergo redox cycling with the intracellular electron-carrier, reduced gluthathione (GSH), to reduce the quinone, and (or) to form a GSH-naphthoquinone complex (conjugate) (Smith et al., 1985). This complex can still undergo redox cycling by forming a semiquinone radical, and to generate reactive oxygen species in the presence of NADPH (Wafer and Sies, 1983). For this reason, toxic doses of naphthoquinones, such as 1,4 naphthoquinone, rapidly cause the depletion of GSH and a rapid rise of the extracellular calcium ion concentration (Thor et al., 1982). The Smith research group observed the formation of

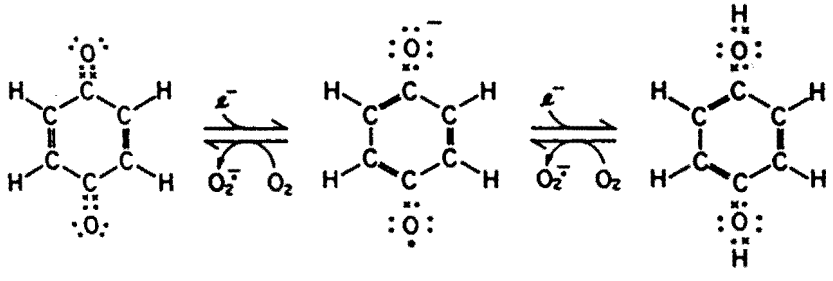

Figure 12. One electron redox cycling of a quinone to its semiquinone radical and hydroquinoe form. The stepwise one-electron reduction of a typical quinone to its semiquinone radical and hydroquinone and their subsequent autoxidation with dioxygen. The total number of electrons per molecule is shown in parentheses. Electrons of carbon and hydrogen atoms are shown × and oxygen atom electrons as ●. Note the unpaired oxygen atom electron in the semiquinone radical. This electron is actually delocalized, giving five resonance forms of the semiquinone radical, but only one is shown here (Smith 1986).

numerous small blebs on the surface of isolated hepatocytes, at a menadione concentration of 50 μM (Thor et al., 1982). These blebs were generated by loss of normal Ca^{2+} homeostasis within the cell. This effect was completely prevented by the presence of GSH. It is likely that the primary site of damage is a thiol group on a Ca^{2+} transport protein found within the hepatocyte (Moor et al., 1976). These naphthoquinones inhibit Ca^{2+} sequestration in mitochondria and ER by oxidation of endogenous thiol groups.

The redox potential for quinones is described by the Nerst equation as follows:

$$E=E_0 +A\ln([Q_{ox}]/[Q_{red}]) \qquad (13)$$

The quinone-quinol system possesses a positive redox potential, and can oxidize another systems having a lower redox potential.

In this thesis, most experiments were carried out using of 1,4-naphthoquinone. It is a potent generator of superoxide in the presence of NADPH, and it is also one of the most cytotoxic quinones. 1,4-naphthoquinone (1,4 NQ), as well as 1,2-naphthoquinone (1,2 NQ) and other 1,4-naphthoquinones such Vitamin K_1 and Vitamin

Table 2 Redox potentials of several quinones
(Modified form Morton. R. A. 1965)

QUINONE	E_0 (V)	pH
1,2-naphthoquinone	0.576	7.0
1,4-naphthoquinone	0.485	7.0
2-methyl-1,4-naphthoquinone	0.422	7.0
2-hydroxyl-1,2-naphthoquinone	0.358	7.0
Anthraquinone	0.154	7.0
Anthraquinone-2-sulfonate	-0.225	7.0

K_3 (menadione) (Cohen, et al., 1983; d'Arch Doherty, et al., 1984; Cosby et al., 1975), are found to be selectively toxic to human tumor tissue. They are the quinone-semiquinone metabolites of 1-Naphthol, a useful anticancer agent. Up to 86% of the naphthol was converted to a 1,4-naphthoquinone in the presence of NADPH under optimal conditions for the NADPH-dependent reaction (Fluk et al., 1984). It is believed that the relatively nontoxic phenols of 1-naphthol are metabolized to redox-cycling quinone metabolites in tumor cells (Smith et al., 1985). On the other hand, 1,4NQ inhibits electron transfer in mitochondria by inhibiting electron transport from NADH (Phelps it al., 1975). It also inhibits superoxide dismutase at concentrations below 100 μM (Smith et al., 1985). In contrast, 1,4NQ and menadione stimulate NADPH oxidation (Talcott et al., 1985).

Fritsch and co-workers reported that there were minimal differences in unpaired electron distributions between 1,4NQ and the various K vitamins (K vitamins belong to the 1,4-naphthoquinone family). These results demonstrated there are no important differences in the chemical reactivity of the aromatic portions of the molecules, regardless of additional large side chains. However, the electron transfer rate of 1,4 NQ is much faster than other 1,4-naphthoquinones (Fritsch et al., 1967).

Guohua Liu and his colleagues reported that 1,4NQ at concentrations <2μM selectively oxidized hyperreactive sulfhydryls on RyR1 (subunit) and triadin, without altering the function of Ca^{2+}-Mg^{2+}-ATPase. Pre-treatment of SR membranes with 1,4NQ (40 pmol/μg) dramatically enhanced the formation of a cross-linked high

molecular weight complex (HMWC), reducing the intensity of the bands at M_r 360,000 (RyR1) and M_r 95,000 (triadin) on nonreduced SDS gels. Even at low Ca^{2+} concentrations (nM), which normally favors channel closure, 1,4NQ still stabilizes the formation of a HMWC and promotes channel activity. This demonstrates that 1,4NQ directly and selectively oxidizes hyperreactive sulfhydryls on RyR1 and triadin. This group also observed that 1,4NQ induces Ca^{2+} release from skeletal SR vesicles without inhibiting Ca^{2+} pump activity (Liu et al., 1984, Liu et al., 1985). These results provided evidence of an important functional interaction between these two triadic proteins.

CHAPTER 3

SPECTROPHOTOMETRIC ASSAY OF 1,4NQ STIMULATING Ca^{2+} EFFLUX

In this chapter, it is shown that 1,4NQ stimulates Ca^{2+} release from skeletal muscle SR. The Ca^{2+} efflux was measured spectrophotometrically by the method described in Chapter 2. 1,4NQ (5 to 400 μM) was found to activate the CRC, while the reduced quinone was not found to activate the channel. Maximum dose dependent release rates were recorded. Ruthenium red and reducing agents, such as DTT and GSH , inhibited the effect of 1,4NQ on the CRC.

1,4NQ stock solutions were made in DMSO, at concentrations of 10, 20 and 40 mM. Control experiments with DMSO showed that DMSO at less than 5% had no effect on the Ca^{2+} release mechanism of SR.

1 1,4NQ STIMULATED Ca^{2+} EFFLUX

1,4NQ induced Ca^{2+} efflux from actively loaded SR vesicles in a concentration dependent manner. The measurements were carried out with a the dual wavelength spectrophotometer as described in Section 4 of Chapter 2.

As shown in Fig. 14, 1,4NQ stimulated Ca^{2+} release from actively loaded SR vesicles. After addition of 1,4NQ, the maximum Ca^{2+} release rate was achieved in about one minute. No visible Ca^{2+} release was observed when the 1,4NQ concentration was less than 2 μM. The Ca^{2+} release rate did not saturate at a 1,4NQ concentration as high as 300μM. Compared to doxorubicin, an anthraquinone that acts as a powerful Ca^{2+} release inducing agent, 1,4NQ was considerably less effective (1/10 the release rate) in stimulating Ca^{2+} release from SR vesicles.

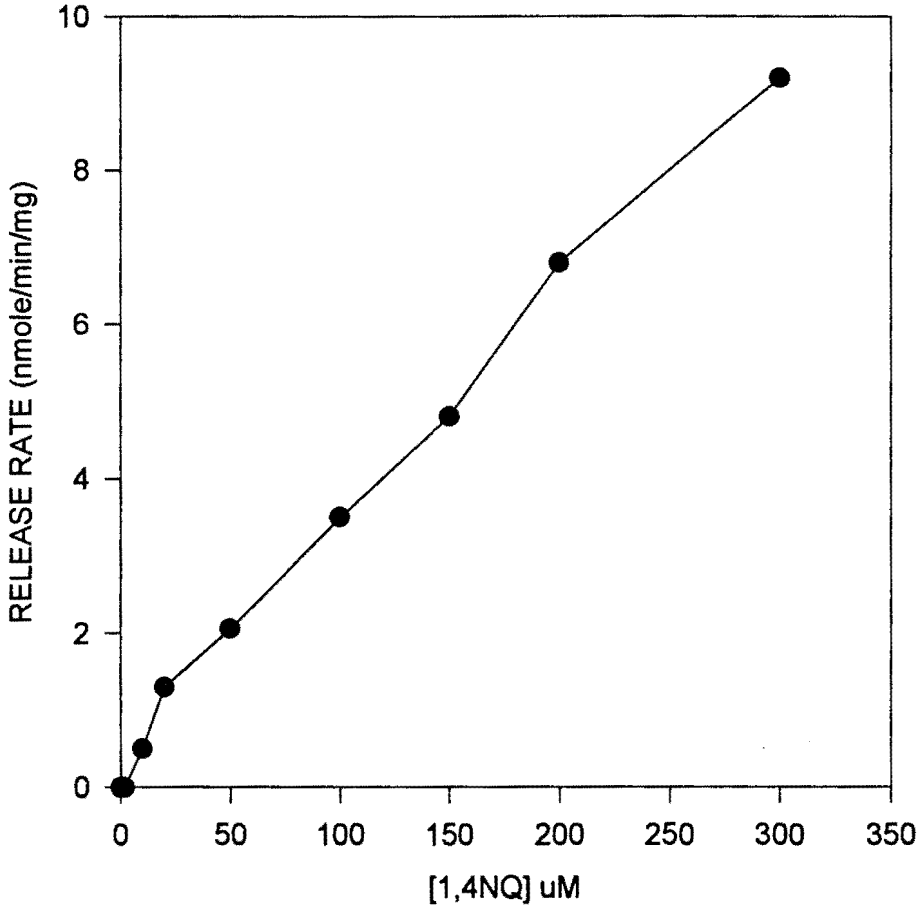

Figure 13. Maximum Ca^{2+} release rate as a function of 1,4-naphthoquinone concentration. These experiments were performed in the presence of 200 μM APIII, 100 mM KCl and 20 mM Hepes, pH 7.0, at room temperature. The release rates were computed from the maximal Ca^{2+} release rate and normalized to the protein concentration. Ca^{2+} uptake (~37μM) was initiated by the addition of 1mM MgATP. Upon completion of Ca^{2+} uptake, the free calcium concentration was measured, and various concentrations of 1,4NQ were added. The extravesicular free Ca^{2+} concentration was recorded by measuring the differential absorbance of APIII at 720 nm and 790 nm. These experiments were repeated twice.

In all of the assays carried out in Fig. 14, the amount of Ca^{2+} actively accumulated by the SR (38 ± 1 μM) and the free Ca^{2+} concentration upon addition of 1,4NQ (3-7 μM) were very similar. The control trial showed that the extravesicular free Ca^{2+} concentration was stable within at least 50 minutes after completing uptake, in the absence of 1,4NQ, which is in excess of the amount of time required for the Ca^{2+} release process.

The standard deviation associated with each of the data points shown in Fig. 14 is approximately 0.5 nmole/min/mg, with the exception of the release rate reported at 300 μM 1,4NQ, in which the error is ~2.1 nmol/min/mg.

2 THE EFFECT OF REDUCING AGENTS ON Ca^{2+} TRANSPORT

Pretreatment of 1,4NQ with the reducing agents GSH or DTT, or addition of the RyR inhibitor ruthenium red, completely inhibited 1,4NQ induced Ca^{2+} release from SR vesicles. 1,4NQ was incubated with GSH (2mM) or DTT (0.2 mM) for 5 minutes at room temperature. Following ATP dependent Ca^{2+} uptake, 0.1 mM reduced 1,4NQ was added to the cuvette. No visible increase in the extravesicular free Ca^{2+} level was detected in 5 minutes. These experiments demonstrated that the reduced form of 1,4NQ was ineffective in activating the CRC from SR.

2.1 Reduced 1,4NQ Inhibits Ca^{2+} Release

As shown in Fig. 14 and Table 3, the reducing agents GSH (0.8 mM) and DTT

(0.2 mM) alter the spectral characteristics of 1,4NQ and 1,2NQ. 1,4NQ (50 μM) has three aborbance maxima at 226 nm, 252 nm, and 342 nm. When 0.8 mM GSH was added to the solution, the 342 nm peak was shifted to 316 nm, which reflects to the reduction of 1,4NQ to its hydroquinone form (Daglish 1950, Harayama 1971). A weak maximum absorbance at 420 nm, which does not exist in the spectrum of the reduced 1,4NQ by dithionite, a strongest reducing agent in existing, is probably caused by the charge-transfer reaction which results in a small fraction of quinone-GSH-complex. DTT (200μM) also shifted 252 nm to 256 nm. The shifting at 342 nm in wavelength is caused by reduction of the quinone, while the weak peak at 420 nm is probably due to a charge transfer of from GSH or DTT to quinone to form complex. A parallel experiment was carried out by adding dithionite to the medium to reduce 1,4NQ to its hydroquinone form, a very similar spectrum was obtained except no maximal absorbance at 420 nm was observed.

Conditions were maintained identically for all experiments in this section. 1,4NQ was incubated with GSH or DTT for 5 minutes at room temperature. When the loading of Ca^{2+} was complete and the signal was stable, 100 μM 1,4NQ+GSH/1,4NQ+DTT (by 2mM GSH, or 200 μM DTT) was added to the cuvette. No visible increase in the extravesicular free Ca^{2+} level was detected in 5 minutes. This demonstrated that activation of the CRC was totally inhibited by the reduced form of 1,4NQ.

Table 3. Absorbance maxima of naphthoquinones in the oxidized and reduced states. Spectra of 1,4 and 1,2NQ (50 μM), yielded absorbance maxima at the wavelengths shown. The addition of GSH (0.8 mM) or DTT (0.2 mM) resulted in the altered spectral characteristics shown. Data was derived from spectrum shown in Fig. 14.

Quinone	Wavelength (nm)
1,4NQ	226, 252, 342
1,4NQ+GSH	228, 244, 316
1,4NQ+DTT	226, 242, 318
1,4NQ+dithionate	226, 242, 322
1,2NQ	226, 252, 346
1,2NQ+GSH	232, 308, 332
1,2NQ+DTT	232, 332

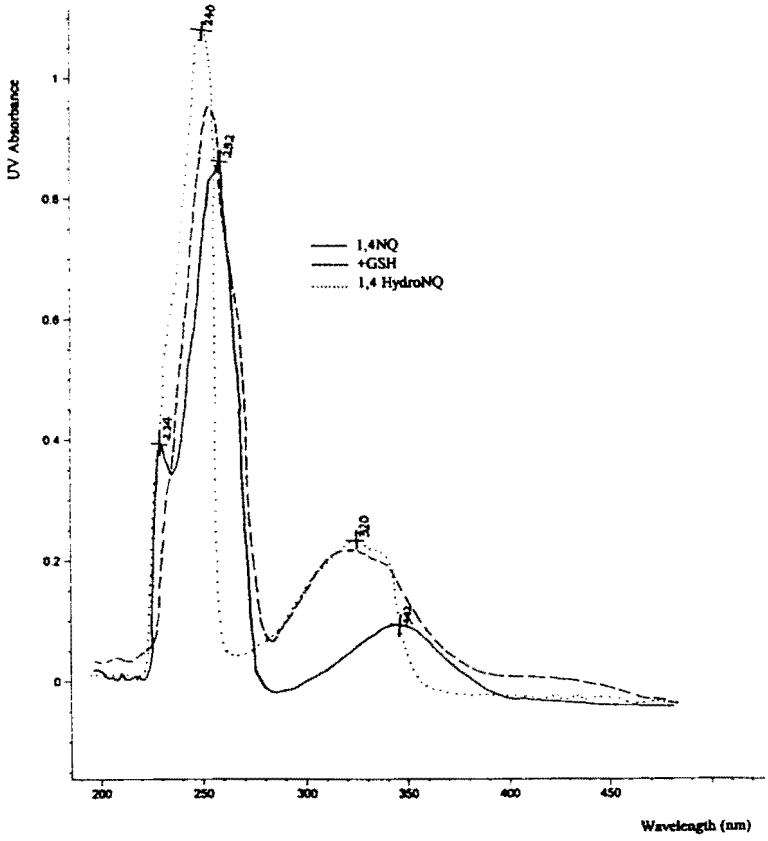

Figure 14. The spectra of 1,4NQ and reduced quinone (GSH, dihydroxylnaphtholane). DMSO was scanned as background for 50 μM 1,4NQ or 1,4-dihydroxylnaphtholane (1,4hydroNQ) spectra, and DMSO plus 0.8 mM GSH was scanned as background for NQ+GSH spectra.

2.2 Reducing Agents and Ruthenium Red Reversed Ca^{2+} Release

Reducing agents, such as GSH and DTT, and the CRC inhibitor ruthenium red inhibited Ca^{2+} release from actively loaded SR vesicles. Following active uptake of Ca^{2+} by SR vesicles, reducing agents were added to the assay medium either before or after the addition of 1,4NQ.

In one set of experiments, 100 μM 1,4NQ was added to SR vesicles following Ca^{2+} uptake stimulated by ATP. Following completion of the Ca^{2+} release phase, 2mM GSH was added to the assay medium, and approximately 32% of the released Ca^{2+} was actively reaccumulated by the SR. DTT (200 μM) was slightly more effective in reversing the release of Ca^{2+} induced by 1,4NQ (~45% of released Ca^{2+} reaccumulated by the SR). In a second set of experiments, CRC inhibitors were added during the Ca^{2+} release phase induced by addition of 100 μM 1,4NQ. GSH (2mM) abruptly stopped Ca^{2+} release induced by 1,4NQ. While ruthenium red (10 μM) stopped release and closed the release mechanism down, such that 80% of the released Ca^{2+} was subsequently taken back up into the SR.

If DTT (200 μM) or ruthenium red (10 μM) was separately added to the solution prior to the addition of 1,4NQ, they completely prevented 1,4NQ from inducing Ca^{2+} efflux. However, if GSH was added to the assay medium, prior to addition of 1,4NQ, the rate of release induced by 1,4NQ was decreased, but not completely inhibited.

3 Ca^{2+} RELEASE STIMULATED BY OTHER QUINONES

Other quinones were also found to stimulate Ca^{2+} efflux from SR vesicles. Naphthoquinones such as 2-methyl-1,4-naphthoquinone (menadione), 2-hydroxyl-1,4-naphthoquinone, 1,2-naphthoquinone, and some anthraquinones, such as anthraquinon-1-sulfonate and anthraquinone-2-sulfonate, were observed to activate. However, none of these compounds were as efficient as doxorubicin in stimulating Ca^{2+} release from SR vesicles (Abramson et al., 1988).

4. THE EFFECT OF SUPEROXIDE ON THE Ca^{2+} RELEASE MECHANISM

Since 1,4NQ is a powerful superoxide generator in the presence of NADPH, it is necessary to investigate the possible role of superoxide in activation of Ca^{2+} release induced by 1,4NQ. Superoxide dismutase (SOD) catalyzes the conversion of superoxide radical to peroxide (H_2O_2) and molecular oxygen. Catalase and glutathione peroxidase can eliminate the H_2O_2, and can be used in conjunction with the SOD convert H_2O_2 to H_2O. McMahon and Stern demonstrated that 1,4NQ-2-sulfonate decreased the affinity of SOD for superoxide and of catalase for H_2O_2 in the absence of glucose. The presence of glucose in the incubation medium prevented naphthoquinone-induced enzyme inhibition. Based on this knowledge, experiments were carried out

under conditions in which 10 μg/ml or more of SOD was added either before or after the addition of 100 μM 1,4NQ in the absence or the presence of 5,250 unit/ml catalase, respectively. The suspension buffer contained 200 μM APIII, 100 mM KCl, 20 mM Hepes, and 10 mM glucose. There was no significant change in the percentage of Ca^{2+} release from actively loaded SR vesicles in the presence of one or both of these enzymes. Although a slight variation in the release rate was observed, when one or both of the enzymes were present in the solution, the release rate appears to be independent of SOD concentration (Table 4). This result is consistent with the data from spectra in Fig. 14, which demonstrated GSH reduced 1,4NQ to its hydroquino form which is a stable form of quinone and would not undergo further redox cycling.

Table 4. Ca^{2+} release rate and percentage of Ca^{2+} released in the presence or absence of SOD and catalase. Ca^{2+} was actively accumulated into SR vesicles as described in Fig.13. SOD and or catalase was added at the concentrations indicated. Ca^{2+} release was stimulated by the addition of 100 μM 1,4NQ. The initial Ca^{2+} release rate and the total fraction of actively accumulated Ca^{2+} release was measured.

Release Rate (nmole/min/mg)	Total Release(%)	[SOD] μg/ml	5250 unit/ml Catalase
1.6 ±0.1	23 ±3	0	0
1.4 ±0.2	23 ±1	10	0
1.2 ±0.1	23 ±1	10	+
1.25 ±0.1	19 ±5	20	+
1.33 ±0.2	27 ±3	40	+

CHAPTER 4

EQUILIBRIUM RYANODINE BINDING ASSAYS

There is a strong correlation between the binding of the plant alkaloid ryanodine to mammalian CRC and the functional state of the CRC. In this study ryanodine binding assays were used to understand the interaction between the channel modulator 1,4NQ and the Ca^{2+} channel protein from SR

1. 1,4 NAPHTHOQUINONE INTERACTION WITH THE Ca^{2+} RELEASE CHANNEL

The effects of 1,4NQ on ryanodine binding to the RyR of SR vesicles were examined in the presence of 10 μM Ca^{2+}, an optimal Ca^{2+} concentration for activation

of the channel (Mickelson et al., 1988). As a function of 1,4NQ concentration, ryanodine binding revealed a biphasic behavior. Binding was stimulated at low 1,4NQ concentrations (1-5 μM). However, in the range of 10-50 μM Ca^{2+} binding decreased dramatically, and was totally inhibited at 50μM of 1,4NQ. As shown in Fig. 15, different naphthoquinones such as 1,4NQ, 1,2NQ, 1,4NQ-2-sulfonate, and 1,2NQ-4-sulfonate (data not shown) had similar inhibitory effects at higher concentrations.

The effect of 1,4NQ on ryanodine binding was then examined as a function of Ca^{2+} concentrations. In the absence of 1,4NQ, and at a low concentration of 1,4NQ (5μM), binding was slightly stimulated at <10μM Ca^{2+}, and saturated at >10μM Ca^{2+}. At a high concentration of 1,4NQ (50μM) binding was totally inhibited (Fig. 16). From these results, it is clear that the degree of inhibition caused by 1,4NQ is strongly a function of naphthoquinone concentration. The biphasic modulation by 1,4NQ may very likely be due to at least two different classes of binding sites on the RyR. An activation binding site, which is probably in an aqueous environment, corresponds to low quinone concentration, and an inhibition site corresponds to the high quinone concentration, which is probably located in a less accessible environment. The fact that high quinone concentrations inhibit overall ryanodine binding indicates that there are probably more inhibition sites than activation sites on each RyR.

In control experiments no effects were observed on ryanodine binding or Ca^{2+} transport (data not shown) with as much as 5% DMSO.

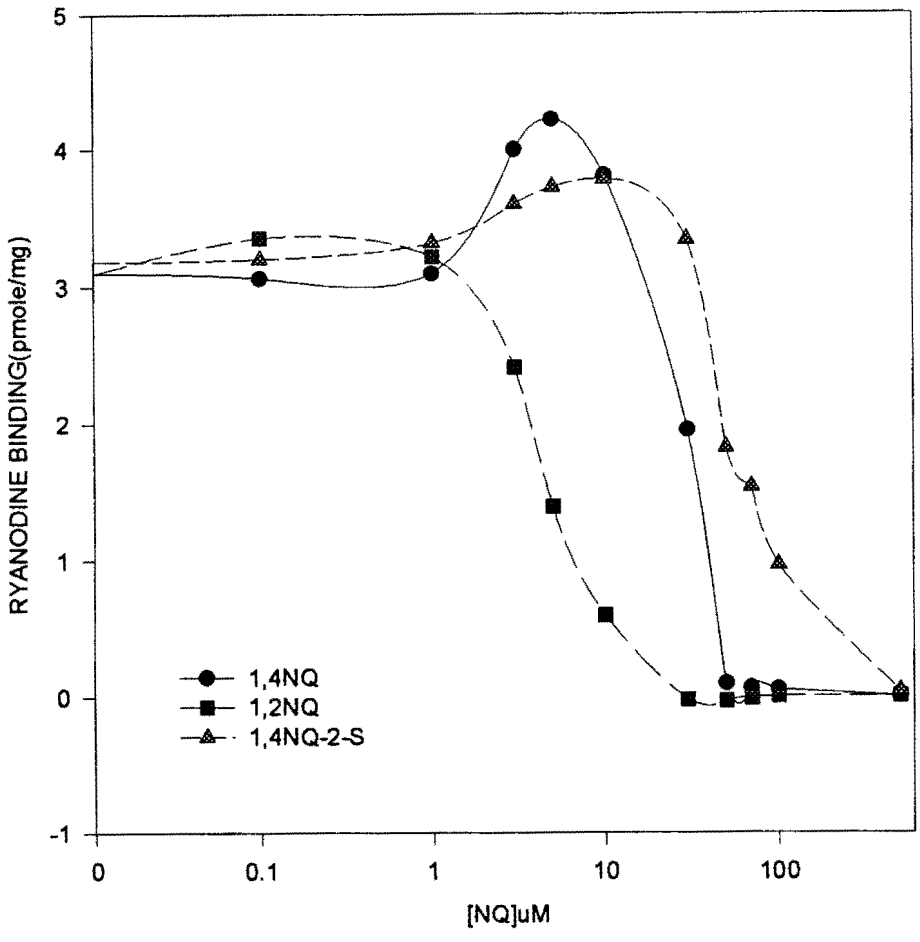

Figure 15. Quinone concentration dependence of ryanodine binding. All experiments were carried out under the same conditions. 0.5 mg/ml rabbit skeletal muscle SR was incubated with concentrations of quinones ranging from 0 - 500 μM in a buffer containing 250 mM KCl, 15 mM NaCl, and 25 mM Hepes, 10 μm $CaCl_2$, pH 7.1, at 37^0C for 3 hours.

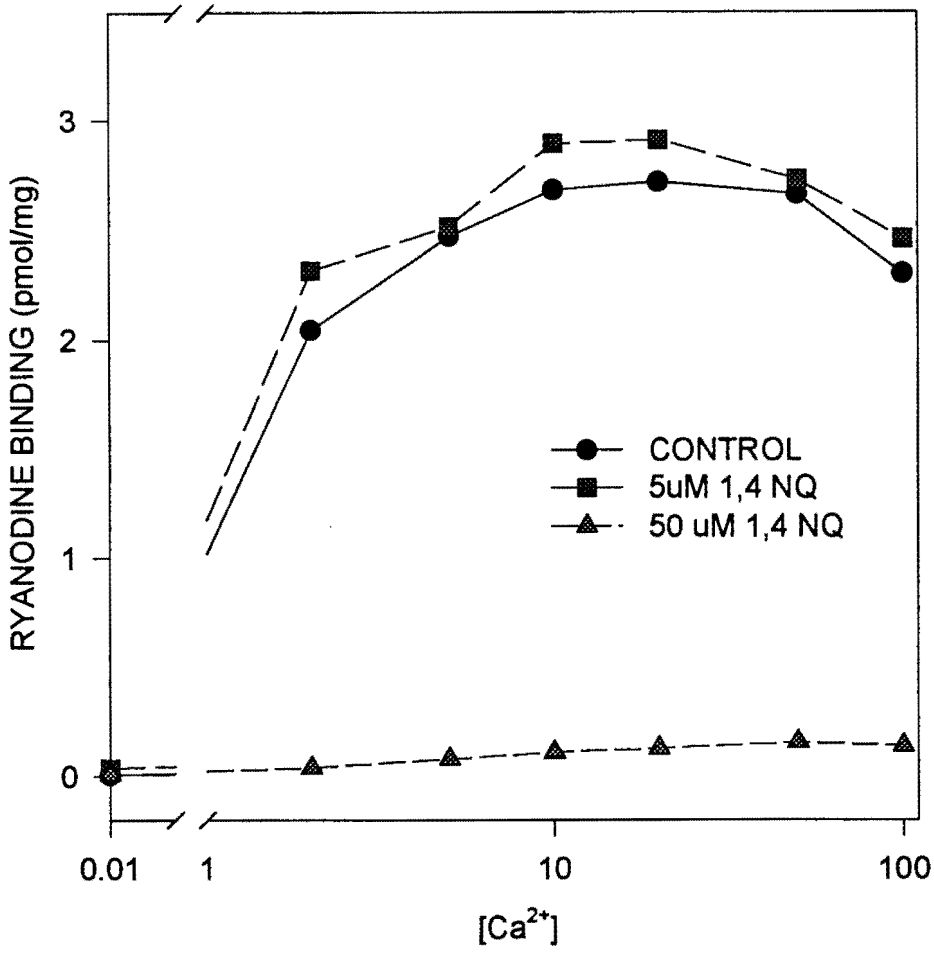

Figure 16. Ca^{2+} dependence of ryanodine binding in the presence of 5μM and 50μM 1,4 NQ. 0.5 mg/ml SR was incubated with or without 5μM or 50 μM 1,4 NQ in a conventional binding buffer for 3 hours at 37°C, pH 7.1. Total free Ca^{2+} in the solution was 62 μM. Different concentrations of EGTA were added to yield the given free Ca^{2+} concentration. Higher Ca^{2+} concentrations (100 μM) were obtained by the addition of appropriate amounts of $CaCl_2$. All 1,4 NQ solutions were diluted from a stock solution of 40 mM in DMSO. The final concentration of DMSO was less than 5% for all samples.

2. REDUCED 1,4NQ DOES NOT INHIBIT RYANODINE BINDING: HILL ANALYSIS

In the Ca^{2+} transport assay, the finding that 1,4NQ induced Ca^{2+} efflux by activating the CRC, while the reduced quinone did not implies that the functional modulation of the Ca^{2+} release channel is operated by a redox mechanism.

Important parameters, such as the IC_{50}, the degree of cooperativity *n* (Hill constant), and the affinity of activator/inhibitor, can be obtained from a Hill analysis of a concentration dependent ryanodine binding assay. In equilibrium ryanodine binding experiments, reduced 1,4NQ, (1,4NQ pre-treated with 2mM GSH or 200 μM DTT), was observed to diminish the inhibition caused by 1,4NQ (Fig.17A). GSH, a physiologically relevant thiol reducing agent (Zable et al., 1997, Smith et al., 1985), was more effective than DTT in reversing the inhibitory action of 1,4NQ. GSH raised the IC_{50} from 20 μM to 53 μM 1,4NQ (Fig. 17B), while DTT (0.2 mM) only raised the IC_{50} from 20 μM to 32 μM.

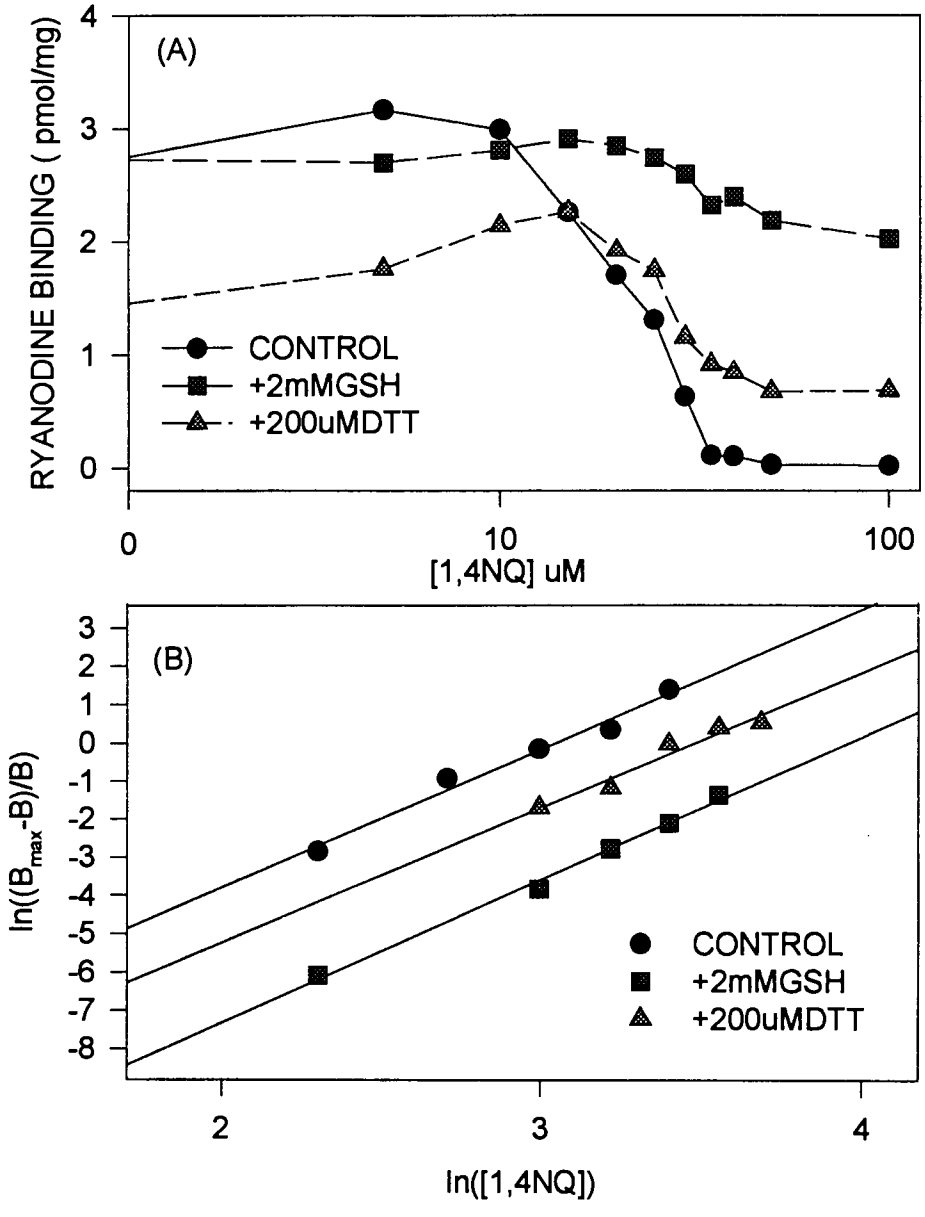

Figure 17. GSH and DTT decreased the inhibition of ryanodine binding induced by 1,4NQ. 2mM GSH or 200μM DTT was pre-incubated with 1,4 NQ at room temperature for 5 minutes to reduce 1,4NQ. 0.5 mg/ml SR was then incubated with 1,4NQ or reduced 1,4NQ in a conventional binding buffer for 3 hours at 37°C. The control points were obtained incubation in the absence of 1,4NQ in the absence of reducing agents. The Hill constant *n* and IC_{50} were calculated by a linear regression program. For control, IC_{50} = 20 μM, *n* = 3.6. For +GSH, IC_{50} = 53μM, *n* = 3.7. For +DTT, IC_{50} = 32 μM, and *n* = 3.5. (A) ryanodine binding versus concentrations of 1,4 naphthoquinone. (B) the Hill plot for the data from figure (A).

The Hill constants, *n*, under each condition, were similar to one another, at 3.6, 3.7, and 3.5 for the control, GSH, and DTT, respectively. This demonstrates that reducing agents effect the degree of sensitivity to inactivation by 1,4-naphthoquinone, but do not effect the degree of cooperativity of the naphthoquinone interaction with the receptor.

3. 1,4NQ DECREASES THE RYANODINE BINDING AFFINITY: SCATCHARD ANALYSIS

The Ca^{2+} transport assay showed that 1,4NQ interacted with the ryanodine receptor by inducing Ca^{2+} release from SR vesicles and by decreasing ryanodine binding to the receptor. A Scatchard analysis was used to provide more direct and detailed information on how this naphthoquinone affects the behavior of ryanodine binding to the RyR.

The Scatchard experiment was carried out under the conditions described in Chapter 2. The results showed that in the presence of 10 μM 1,4NQ and 1,2NQ, ryanodine binding to skeletal muscle SR decreased by ~50% over the control (Fig.18). It also showed that 1,2NQ was a more potent inhibitor of ryanodine binding than 1,4NQ. From the Scatchard plot, the binding constant, K_d, and the maximal number of binding sites, B_{max}, were obtained. It was found that in the presence of these two naphthoquoinones the K_d remains unchanged (Table 5). However, the quinones did decrease B_{max} by ~55% for 1,4NQ and ~60% for 1,2 NQ, compared to the control. By

definition, $K_d = k_{-1}/k_{+1}$. If the rate of association, k_{+1} is altered by 1,4NQ, the rate of dissociation, k_{-1}, must be altered in a similar manner.

The decrease in B_{max} induced by 1,4NQ is probably caused by an inactivation of the receptor, and a loss of binding sites.

Table 5: 1,4 and 1,2NQ modulate binding characteristics to the ryanodine receptor of skeletal muscle SR. Results were obtained from linear regression of the data in Fig. 18. The slope of the linear regression yields the K_d and the x-intercept is B_{max}.

Conditions	K_d (nM)	B_{max} (pmol/mg)
Control (10 μM Ca^{2+})	9.8	4.7
+ 10 μM 1,4 NQ	9.9	2.5
+ 10 μM 1,2 NQ	10.9	1.8

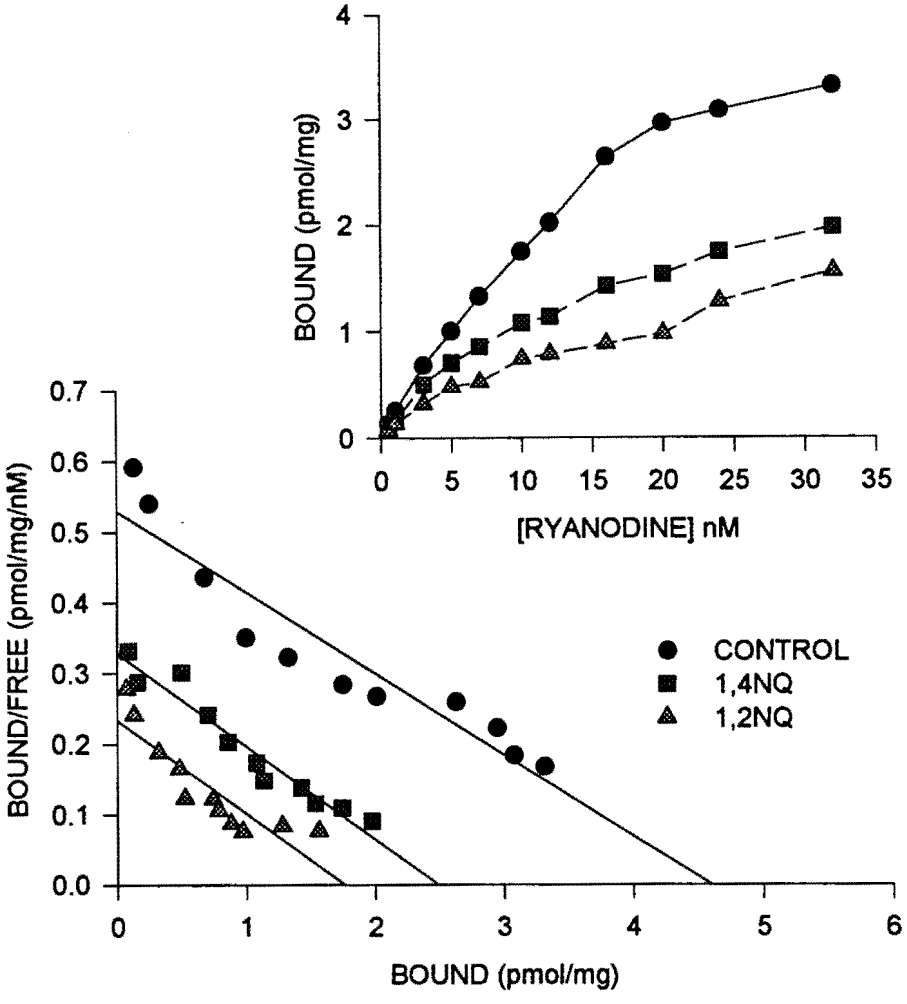

Figure 18. Scatchard analysis of 1,4NQ and 1,2NQ (10μM) inhibition of ryanodine binding. Equilibrium binding was carried out with 0.5 mg/ml rabbit skeletal muscle SR incubated at 37^{0}C for 3 hours in a buffer containing 10 μM $CaCl_2$, 250 mM KCl, 15 mM NaCl, and 25 mM Hepes in the presence of 0.5 nM [^{3}H] ryanodine and varying total ryanodine concentrations from 0.5 to 32 nM. Non-specific binding was obtained with a 3000 fold excess of cold ryanodine. The slopes and intercepts were obtained by linear regression. (A) Ryanodine binding versus various ryanodine concentrations in the absence and presence of 1,4 NQ and 1,2 NQ. (B) Scatchard plot for (A).

CHAPTER 5

DYNAMIC RYANODINE BINDING ASSAYS

In the previous ryanodine binding assays, binding results were obtained at a point of saturation, after 3 hours incubation at 37^0C. There is no information available at this point in time to reveal the dynamics of ryanodine binding in the presence of a modulator such as 1,4NQ. To uncover this information, association and dissociation experiments were performed as a function of time.

1 TIME DEPENDENT ASSOCIATION EXPERIMENT

Association experiments were performed as a function of time, as described in Chapter 2.

1.1 Association of Ryanodine was Biphasic in the Presence of 1,4 NQ

The results shown in the following figures and tables reveal two very important properties. First, ryanodine binding displays two distinct phases when SR is incubated with 1,4NQ. Binding is stimulated by 1,4NQ at early time points (phase 1), but is gradually inhibited as incubation times increase (phase 2). Second, both the stimulation and the inhibition of binding appears to be dependent on 1,4NQ concentrations.

At the earlier times (0-30 minutes), ryanodine binding was stimulated at all 1,4NQ concentrations, but both maximum amount of binding and the time range of the stimulation declined with increasing quinone concentration. At later times (30-180 minutes), binding was inhibited by 1,4NQ in a concentration dependent manner (Fig. 19). At 180 minutes, binding decreased from 2.6 pmol/mg to 1.6 pmol/mg at 10 μM 1,4NQ, and to 0.1 pmol/mg at 50 μM (Table 6, Figs.19 and 23). These results strongly suggest that there are at least two classes of functional sites on the RyR of the SR membrane. One class may be activated by the presence of the 1,4NQ, while the other class of lower affinity was inhibited by 1,4NQ. This is consistent with results presented in Fig. 15, in which there appears to be an activation site stimulated at low 1,4NQ concentrations, and an inhibition site occupied at higher concentrations of 1,4NQ.

The presence of 1,4 NQ increases the initial rate of ryanodine binding to the RyR in the early phase of binding, from 0.06 pmol/mg/min (control) to 0.133 pmol/mg/min (mean of rates for 10 μM, 30 μM, and 50 μM 1,4NQ) in the first 6 minutes (Table 7). This demonstrates an increase in the probability of finding the RyR

in an open state in the presence of 1,4NQ. However, there is no appears correlation between increased 1,4NQ concentrations and the initial rate of ryanodine binding. The lack of correlation appears to be caused by the more potent effect of 1,4NQ on phase 2 inhibition of ryanodine binding. As noted in the discussion of Fig. 19, increased 1,4NQ concentrations causes a decrease in the maximum binding and an earlier onset of the time dependent inhibition of binding. It appears as if the increased initial rate of ryanodine binding expected at higher 1,4NQ concentrations is offset by a stimulation of phase 2 inhibition of the receptors. The well defined effects of 1,4NQ on phase 2 inhibition of receptor occupancy is most evident after long incubation times (180 min.- see table 6).

1.2 GSH Reversed the Effect of 1,4 NQ

When 1,4NQ is pretreated with 2 mM GSH, many of the alterations to ryanodine binding are reversed (Fig. 19, 21 B). Most notably phase 2 inhibition induced by 1,4NQ (10 μM, 20 μM, and 30 μM) is totally reversed by pretreatment with GSH. At 50 μM 1,4NQ+GSH, the biphasic time dependent activation followed by inactivation is still evident.

The characteristics of ryanodine binding in the presence of 1,4NQ pretreated with a reducing agent are as follows:

a) The rate of ryanodine binding is less in the presence of 1,4NQ+GSH than in control experiments without GSH and/or 1,4NQ. The reduced 1,4NQ inhibits ryanodine

binding to its receptor.

b) As shown in Fig. 21A, the initial rate of binding of ryanodine at higher NQ concentrations is linearly proportional to the 1,4NQ concentration in the presence of GSH. The reversal of phase 2 inhibition of ryanodine binding linearize the response during phase 1 to activation by 1,4NQ.

c) GSH pretreatment of 10 μM 1,4NQ inhibits the initial rate of ryanodine binding below that of untreated control samples (Fig. 20).

Table 6. The effect of GSH on the characteristics of biphasic ryanodine binding induced by 1,4-naphthoquinone. The control data is from samples not treated with 1,4NQ. Maximal binding occurred during phase 1 (within the first 60 minutes). Results were obtained in three independent experiments. Binding is expressed in pmol/mg.

[1,4NQ] μM	Maximal Binding in initial phase	Binding at 180 minutes	Maximal binding in initial phase in the presence of 2mM GSH	Binding with 2mM GSH at 180 minutes
0	----	2.6±0.2	----	2.5±0.1
10	2.5±0.1	1.6±0.3	----	2.5±0.2
20	1.7	1.0	----	2.3
30	1.6±0.1	1.0±0.1	1.6±0.2	2.2±0.1
50	1.3±0.2	0.1±0.1	1.4±0.2	0.4±0.1

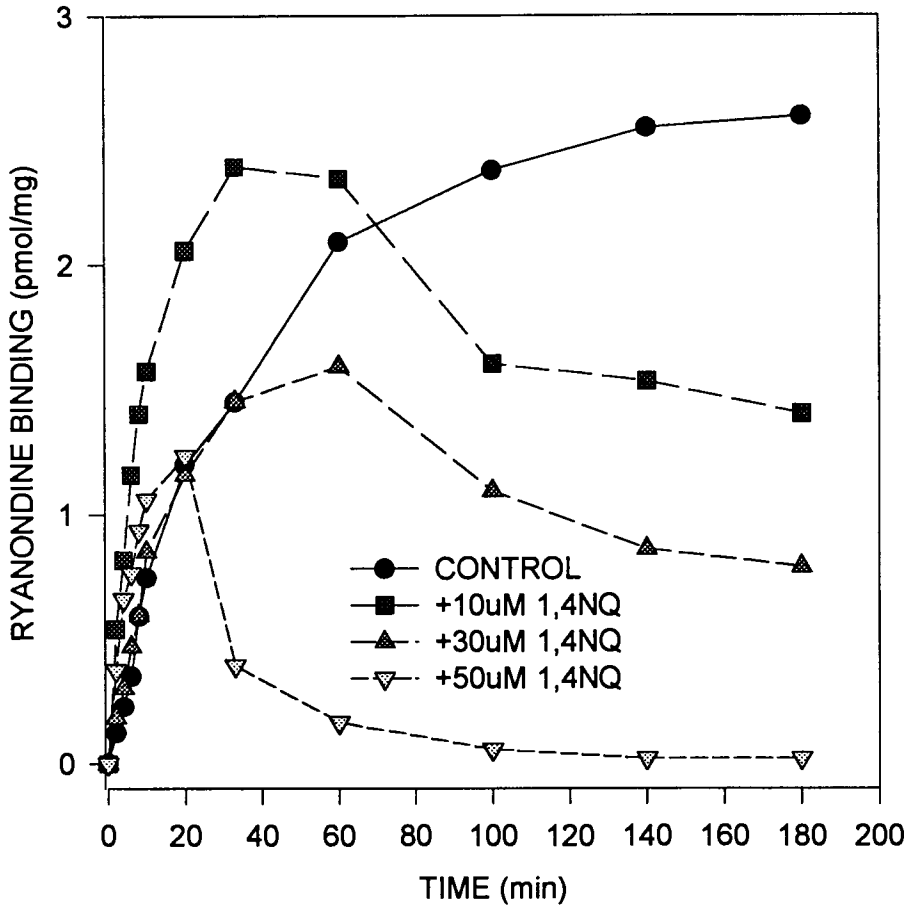

Figure 19. 1,4NQ induced both a stimulation and an inhibition of ryanodine binding to the RyR in a time dependence binding assay. 0.5 mg/ml SR was suspended in a conventional binding buffer as described before with 10 μM Ca^{2+}. The association process was initiated by the addition of suspended membrane to the 1,4NQ solutions. The resulting mixtures were incubated at 37^0C for various time periods. Experiment was repeated 3 time with similar results.

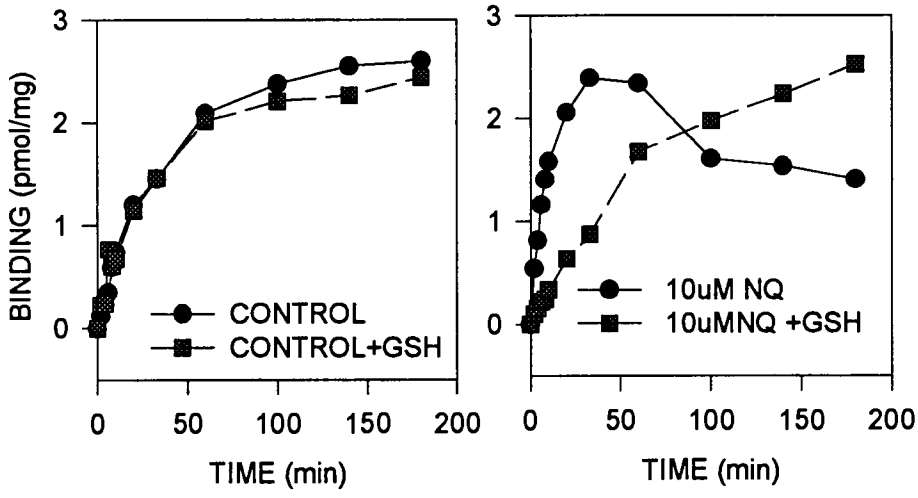

Figure 20. The effects of 2mM GSH on the time dependence of ryanodine binding in the absence and presence of 10 μM 1,4NQ. Data is from Fig. 21 B.

Control experiments with 2mM GSH showed only minimal inhibition of ryanodine binding to the receptor (control and control + GSH, Fig. 20). Addition of 5% DMSO also had no effect on ryanodine binding (data not shown).

Table7. The initial rate of ryanodine binding as a function of 1,4NQ concentration and GSH pretreatment. Data were calculated from the first 4 binding points in the initial 6 minutes of each set from two independent experiments.

[1,4NQ]μM	Initial binding rate (pmol/mg/min)	Initial binding rate (+GSH) (pmol/mg/min)
0 (control)	0.061	0.060
10	0.191	0.037
20	0.105	0.053
30	0.083	0.094
50	0.167	0.171

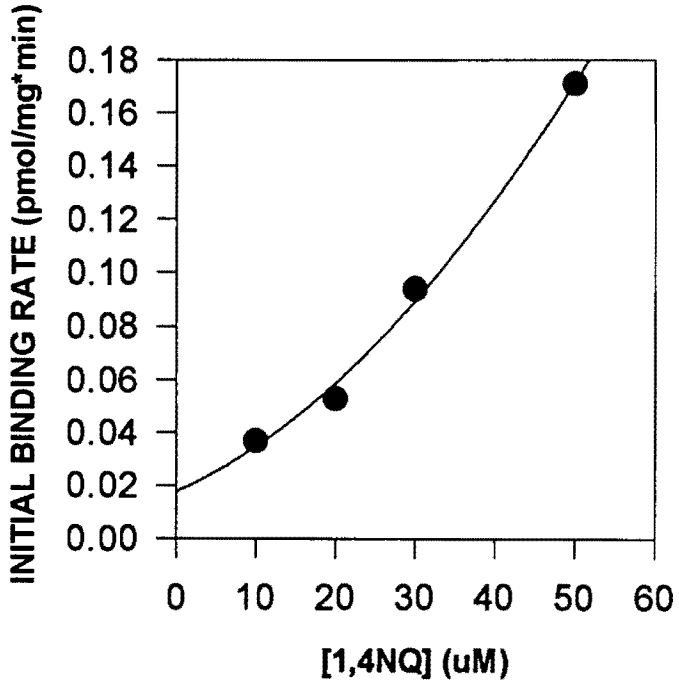

Figure 21 A. Initial rate of binding in the presence of 2 mM GSH. This figure is generated from the data in Table 7.

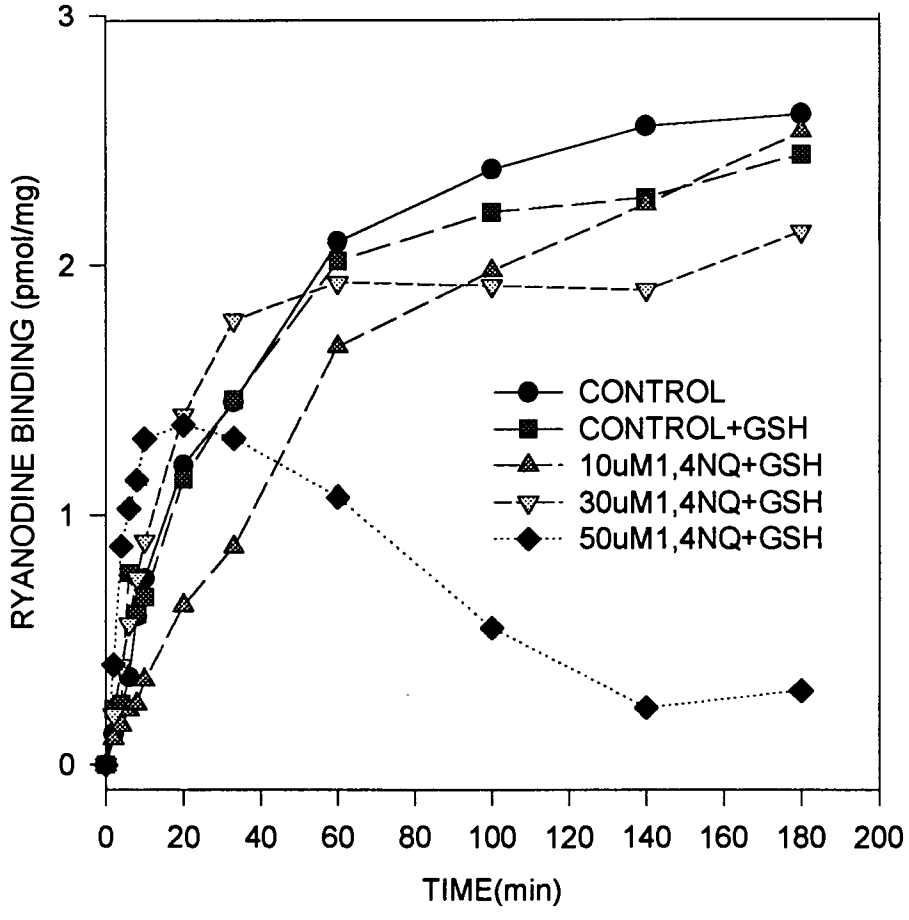

Figure 21 B. GSH reversed the inhibition of ryanodine binding by 1,4NQ. All experiments were carried out with 2mM GSH pretreatment as described in Fig. 22. Experiment was repeated 3 time with similar results.

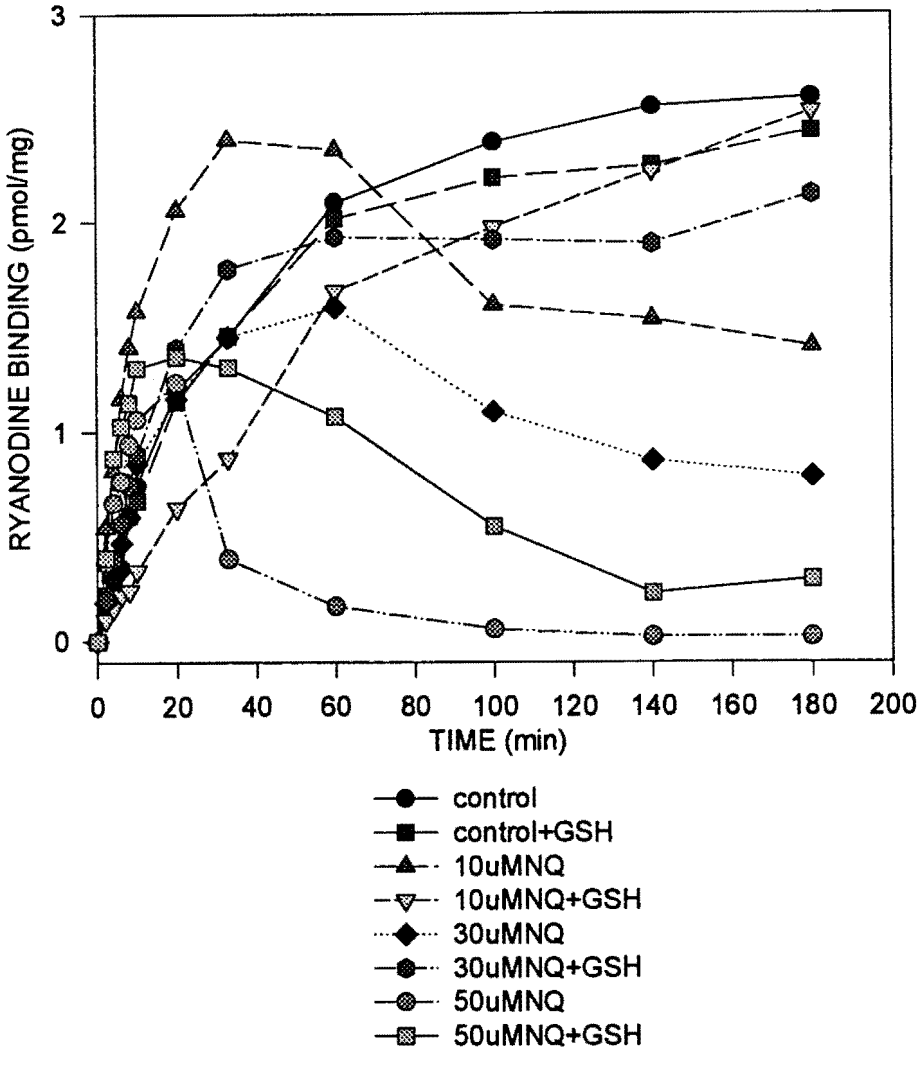

Figure 22. The biphasic effects of 1,4NQ and reduced 1,4NQ on time dependent ryanodine binding. Various concentrations of 1,4NQ were incubated with 2mM GSH at room temperature to reduced quinone to hydroquinone. The SR was added at different times to initiate the association process. The resulting solution were maintained at 37^0C until the last time point was reached. The binding buffer contained 250 mM KCl, 15 mM NaCl, and 25 mM Hepes, pH 7.1. Ca^{2+} was adjusted to 10 μM by the addition of EGTA to the SR solution. EGTA concentrations required to achieve this were calculated by the program BAD. The nonspecific data were taken from first time points. Nonspecific binding was calculated from the t=0 point and was subtracted from all subsequent data points.

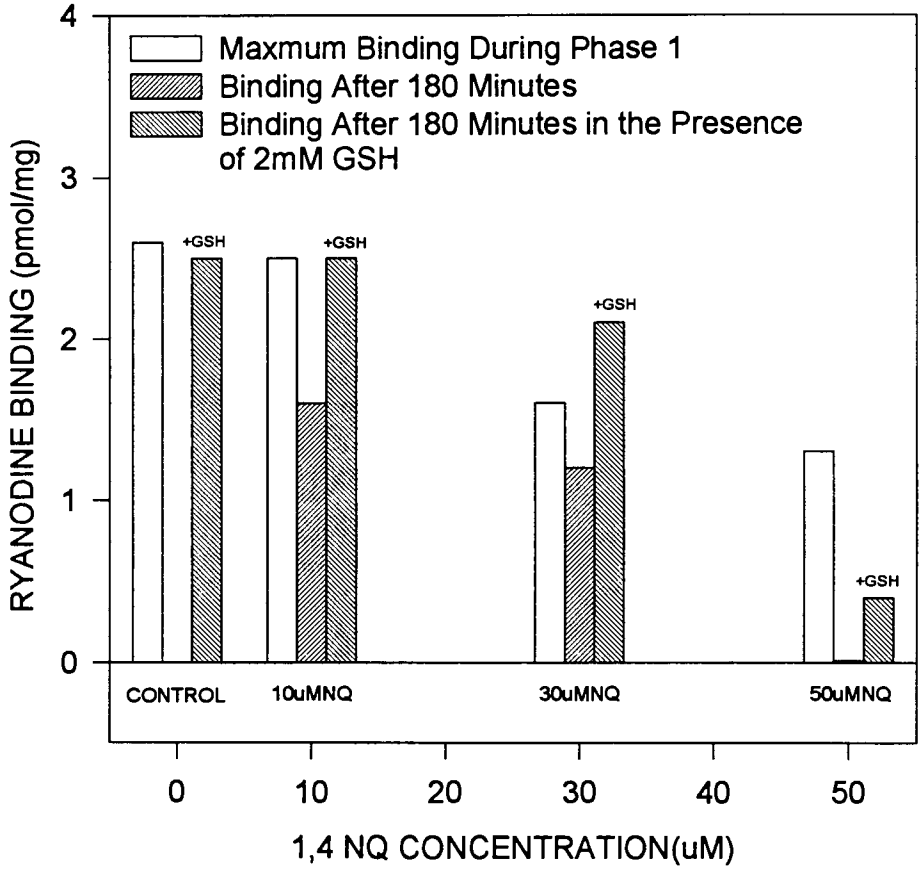

Figure 23. Glutathione prevents naphthoquinone induced inactivation of the RyR. The conditions were the same as those described in Figure 22 and Table 7. Data were the means of 2 independent experiments.

1.3 The apparent Association Rate Constant *K*

The binding data during phase 1 activation of the ryanodine receptor can be fit to the form $B=B_{max}(1-exp^{-Kt})$. By plotting $\ln((B_{max}-B)/B_{max})$ vs. time, the slope ($-K$) was evaluated (Fig. 24A and 24B). The apparent association rate constant is shown in Table 8, as a function of 1,4NQ concentration in the absence and presence of 2mM GSH.

Table 8. The change in the apparent association rate constant *K* for ryanodine binding, caused by 1,4NQ and 1,4NQ+2mM GSH. This graph was generated from the initial data points obtained from two independent experiments. k_{+1} is calculated from the slope of the lines in Fig. 24A and B. The slope is *K*.

[1,4NQ] uM	*K*(1/min)	*K* (+GSH) (1/min)
0	0.0495	0.113
10	0.213	0.0165
20	0.081	0.024
30	0.063	0.048
50	0.170	0.240

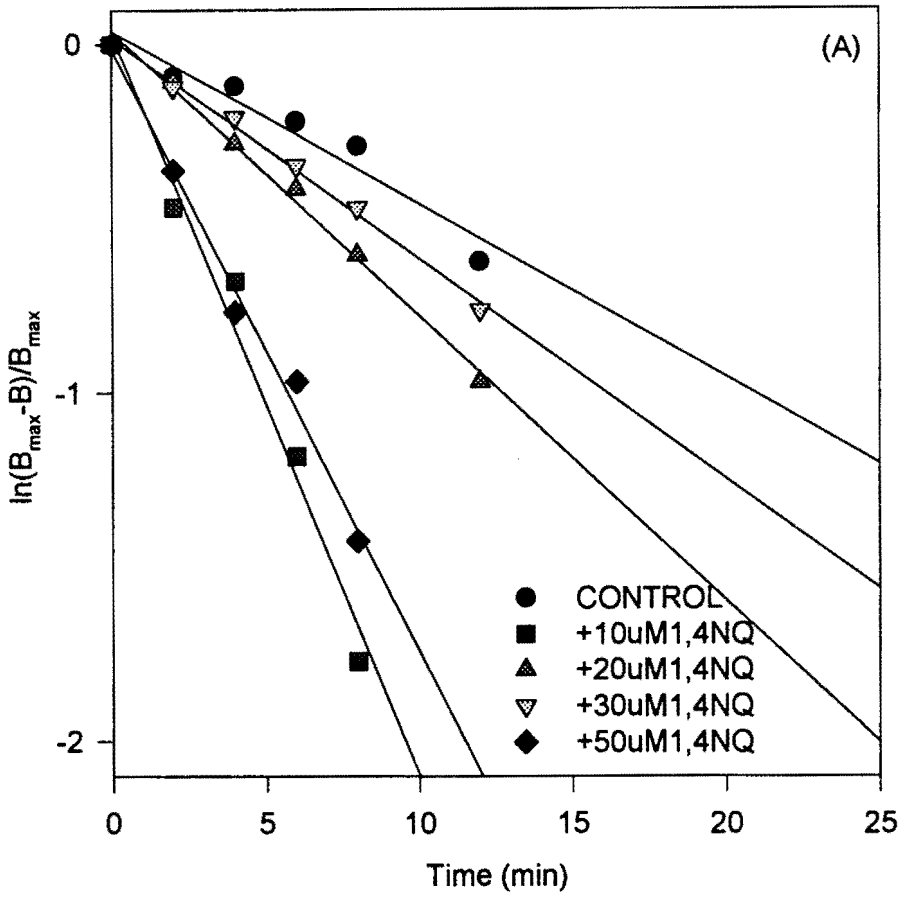

Figure 24 A. The effect of various concentrations of 1,4NQ on the apparent association constant *K*. This graph was generated from the data presented in Fig. 22. The values of *K* which were derived from the slopes of the fitted lines shown, are given in Table 8.

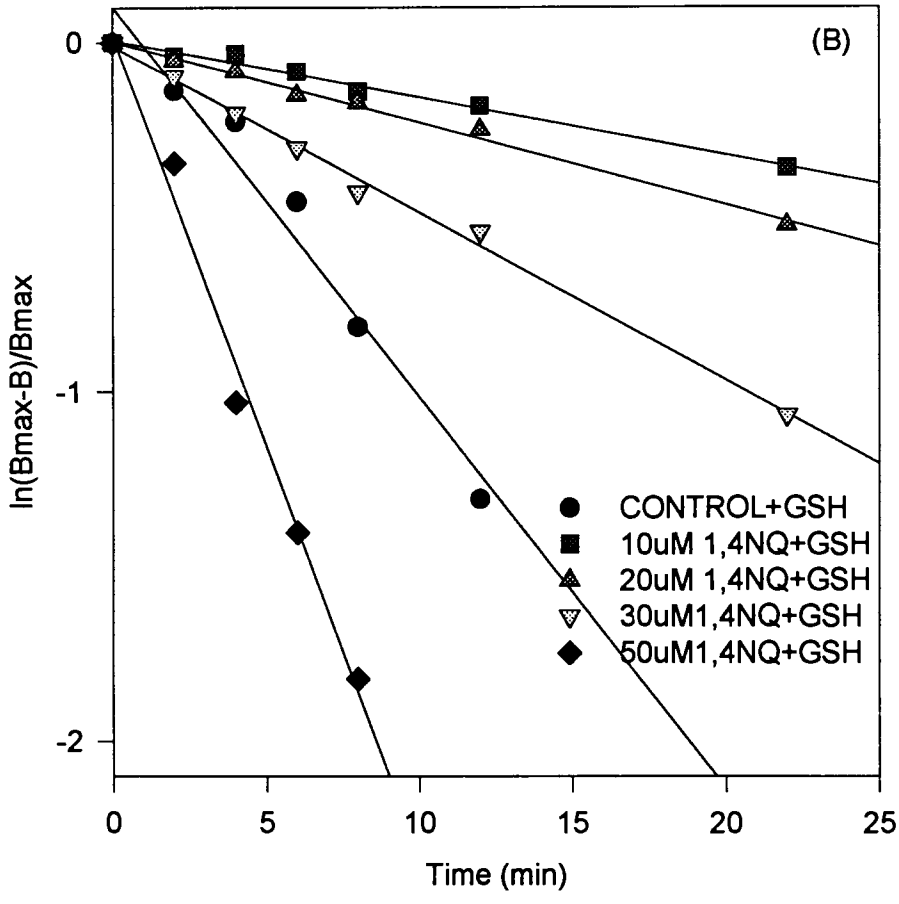

Figure 24 B. The effect of reduced 1,4NQ on the apparent association constant *K*. This graph was generated from the data presented in Fig. 22. The data is plotted as ln $(B_{max}-B)/B_{max}$ vs. time. In graphs A and B, the control samples had no NQ+GSH present. The values of *K* which were derived from the slopes of the fitted lines shown, are given in Table 8.

2. The Dissociation Constant k_{-1}

The dissociation rate constant, k_{-1} was obtained from the time dependence of ryanodine dissociating from its receptor, in the absence and presence of 1,4NQ. If the $\ln(B/B_{max})$ is plotted vs. the time, the slope of the line equals $-k_{-1}$ (Fig. 25). For 1,4NQ, the points at times longer than 100 minutes were not considered. The dissociation rate in the presence of 50 μM 1,4NQ is approximately 2.6 times the rate of dissociation in the absence of naphthoquinone.

The experimental protocol was as described in Chapter 2. The time t = 0 began after 3 hours incubation with ryanodine at 37^0C (without 1,4NQ) when the samples were diluted 100 fold into a buffer containing either 0 or 50 μM 1,4NQ and placed on ice immediately, but the dissociation process is not entirely quenched. This results in a small decrease in ryanodine binding observed for NQ treated SR at t=0 (Fig. 25) between the two data points for this time (see Fig. 25), due to the fact that 1,4NQ causes a faster dissociation. The similarity in initial binding for the control and 50 μM 1,4NQ were due to the absence of 1,4NQ during the 3 hours incubation at 37^0C. determined by the addition of 2mM EGTA to the initial incubation buffer prior to the dilution.

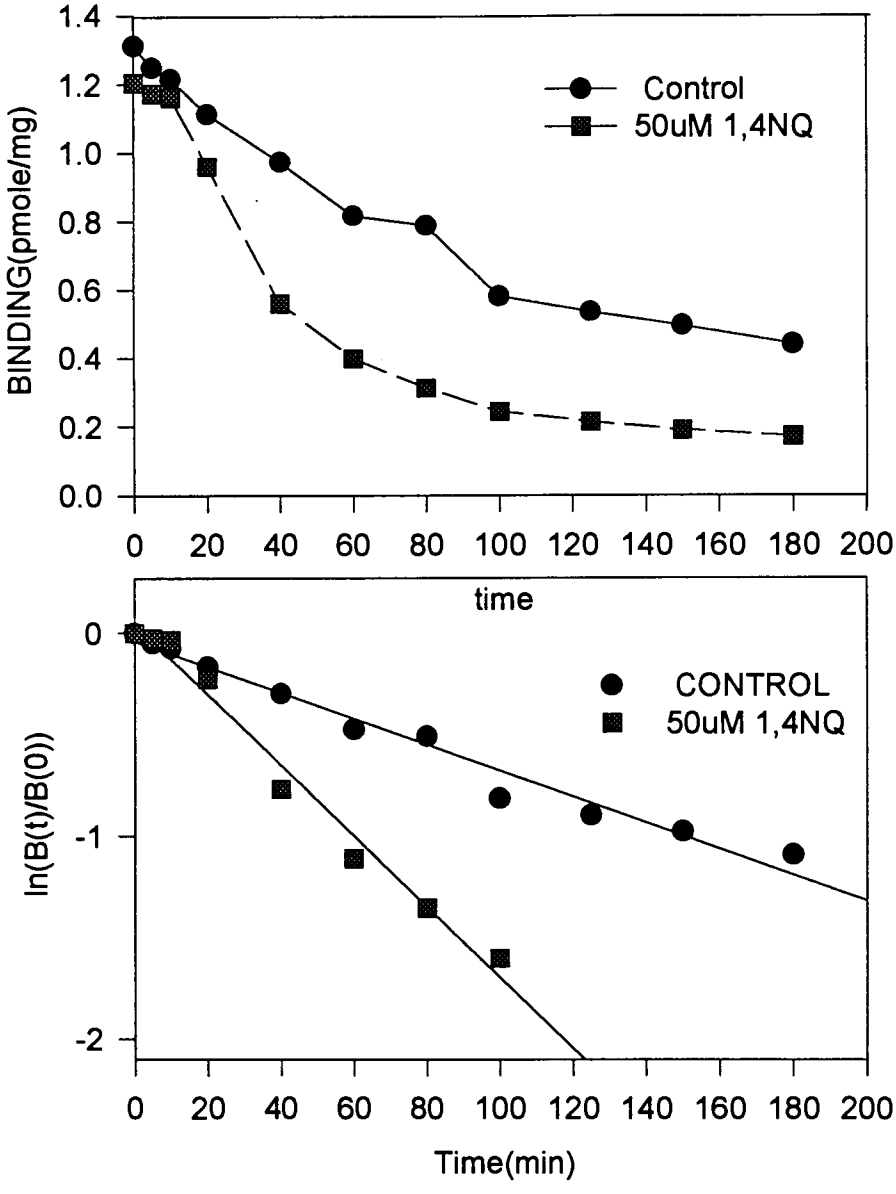

Figure 25. Dissociation of bound ryanodine as a function of time. 5mg/ml SR vesicles were incubated in a solution of 250 mM KCl, 15 mM NaCl, 25 mM Hepes, 5nM ryanodine, and 5nM [^{3}H] ryanodine, pH, 7.1, for 3 hours at 37^{0}C. The free Ca^{2+} concentration was adjusted to 10 μM by the addition of EGTA. Samples were then diluted 100 fold into an identical buffer in the presence of the indicated 1,4NQ concentrations. At each time point, 2ml of the reaction mixtures was taken from the 37^{0}C bath and set on ice to stop the dissociation process.

CHAPTER 6

CONCLUSIONS AND DISCUSSION

Recent evidence from several research groups has revealed that the functional operation of the Ca^{2+} release channel of skeletal SR is modulated by an oxidation-reduction mechanism, in which the oxidation of critical thiols on the RyR leads to the opening of the channel and the reduction of the disulfide formed closes the channel. This hypothesis is supported by the results from experiments presented in this thesis. These results demonstrate that the modulation of channel activity by some reactive sites, on the RyR, is controlled by the cytosolic redox environment. In addition, it is likely that two or three thiol groups on this channel protein are cooperatively involved in the redox reaction to functionally modulate the opened and closed states of the RyR.

The primary results from these experiments are as follows:

1) 1,4NQ, which is believed to selectively oxidize thiol groups, induced a slow, concentration-dependent Ca^{2+} release from actively loaded SR vesicles. The reduced form of this quinone prevented Ca^{2+} release immediately. Combined with the results showing that GSH, DTT, and RR partially reversed Ca^{2+} efflux, and that physiological

concentrations of Mg^{2+} decreased the release rate (data not shown), it is suggested that 1,4NQ interacts with the calcium release channel of SR, thereby activating the channel.

2) Lower 1,4NQ concentrations (<10μM) induced a slight increase in equilibrium binding of ryanodine to the receptor, and higher concentrations (>10μM) effectively inhibited the binding in a concentration-dependent manner. The B_{max}, derived from a Scatchard analysis of binding, showed a 2 fold decrease in the presence of 10 μM 1,4NQ, as compared to the control, with the K_d being unaffected. This information can be interpreted to mean that a large fraction of the calcium release channels present in the solution with 10 μM 1,4NQ were in the closed state, and therefore ryanodine was not able to bind to them. In addition, the presence of Ca^{2+} was necessary for the stimulation of ryanodine binding by 1,4NQ at lower quinone concentrations. In the presence of 5 μM quinone, ryanodine binding showed a similar Ca^{2+} dependence to a control experiment untreated with 1,4NQ. In contrast, binding was inhibited and was independent of the Ca^{2+} concentrations in the presence of 50 μM quinone (Fig. 16).

3) 1,4NQ+GSH reversed the inhibition, of ryanodine binding induced by free 1,4NQ. In quinone concentration-dependent binding experiments, 2mM GSH or 200μM DTT pretreatment did not inhibit binding at high concentrations of the quinone. It is interesting to note that GSH, which is an endogenous reducing agent in the intact SR, exerted a greater effect than DTT, which is a stronger reducing agent. It is probable that GSH reduces the quinone more easily than DTT. The Hill constant (n=3.6)

describing NQ induced inhibition of ryanodine binding for 1,4NQ and 1,4NQ+GSG shows a high degree of cooperativity between the binding sites on each RyR, in the presence of either 1,4NQ or 1,4NQ+GSH. This indicates that the cooperativity between the NQ binding sites on the receptor were consistently high with or without reducing agents. This may be caused by the small fraction of free quinone molecules, which are not reduced by GSH or DTT, interacting with the channel. It is likely that the reduced quinone is not capable of inhibiting the RyR.

4) The data from the dynamic association experiments demonstrated that ryanodine binding to the RyR exhibits two distinct phases, including an initial activation phase (phase 1), in which binding was stimulated by 1,4NQ within 60 minutes of incubation, followed by an inhibition phase (phase 2), in which binding was inhibited at longer periods of time (up to 180 minutes.) Since ryanodine binds to the receptor only when the channel is activated by modulators, the two phases correspond to the channel's opened and closed states, respectively. This suggests two classes of functional sites on the RyR, which modulate channel activity. It can be seen from the binding curve in Fig. 19 that a small concentration of 1,4NQ activates the RyR over the entire time course, but binding is slightly decreases at longer times. However, as the concentration of 1,4NQ increased, the biphasic behavior is more obviously apparent. As the concentration of 1,4NQ increased, the time required for activation and the maximal binding decreased. In phase 2, the inhibition of binding increased with increasing

concentrations of 1,4NQ. At 50 μM 1,4NQ, binding decreased to zero by the end of three hours.

5) The function of the RyR was modulated by a redox mechanism. When 1,4NQ was pretreated with 2mM GSH, the resulting reduced 1,4NQ not only inhibited the initial binding rate in phase 1 (and the apparent association rate constant *K*), but also increased the binding of the second phase dramatically in a 1,4NQ concentration-dependent manner. Smaller ratios of 1,4NQ to GSH caused opposite effects on the two phases (binding decreased in phase 1 and increased in phase 2). It is interesting that 10 μM reduced 1,4NQ not only eliminated the stimulation seen with oxidized 1,4NQ, but it also inhibited Ca^{2+} activation of the channel by decreasing binding below that of the control. This effect is not likely to be due to the presence of 2mM GSH reducing the RyR directly, since this GSH concentration has a very minimal effect on the channel, as shown in Fig. 20 (control + GSH). Increase of the apparent association rate constant and the initial rate of binding in the presence of the quinone, and the decrease of both values in the presence of reduced quinone, indicate that 10 μM 1,4NQ increases the association rate of ryanodine to the ryanodine receptor, while reduced 1,4NQ decreases the association rate. This result also suggests that the reduced 1,4NQ was not able to activate the channel by selectively oxidizing the hyperreactive sulfhydryls in the active site of the RyR.

The above results can be explained as follows: when 1,4NQ, is added to the SR, it interacts first with the easily accessible activation sites by oxidizing sulfhydryls

to disulfide(s). This oxidation activates the channel, thereby increasing ryanodine binding and inducing Ca^{2+} efflux. This is a rapid process, corresponding to phase 1, and suggests that the activation sites face the cytosolic side of the SR membrane. During the redox reaction, the quinone was reduced by GSH. Following activation by 1,4NQ excess quinone can oxidize a second protein thiol site that acts to inhibit the Ca^{2+} channel. Closure of the release channel results in displacement of ryanodine from its high affinity sites (phase 2). Although, reactive oxygen species are hypothetically produced during the quinone reaction with GSH, these species do not seem to be responsible for the effects of 1,4NQ on Ca^{2+} channel function, since neither superoxide dismutase nor catalase affected release induced by 1,4NQ.

When 1,4NQ+2mM GSH is added to SR vesicles, several reactions occur. Both phase 2 inhibition and phase 1 activation of ryanodine receptor binding are inhibited. The reversal of both of these effects by the reducing agent, GSH, strongly suggests that 1,4NQ interacts with the RyR by an oxidation reaction.

The most obvious change to the time dependence of 1,4NQ induced ryanodine binding caused by GSH is the loss of phase 2 inhibition evident at all but the highest concentration of 1,4NQ. At 10 μM 1,4NQ+GSH, the rate of binding is less than that of the control in which neither 1,4NQ nor GSH are present. It appears as if the reduced form of 1,4NQ not only is ineffective in stimulating ryanodine binding, but that it also actually inhibits the receptor. As the concentration of the 1,4NQ is increased in the presence of GSH, the rate of ryanodine binding increases in a linear

fashion. Although there is no direct evidence to support this hypothesis, it appears that as the 1,4NQ concentration increases in the presence of GSH, a small fraction of the 1,4NQ remains free and is able to activate the receptor. Also, with the loss of phase 2 inhibition, the response to activation caused by free 1,4NQ is more evident.

There are several differences between the transport assays and the ryanodine binding assays that are important. The ryanodine binding assays are carried out at 37^0C in the absence of Mg^{2+} , in a high salt buffer (250 mM KCl). Due to the slow kinetics of ryanodine binding, these assays are carried out over a long time period - 3 hours. The Ca^{2+} transport assays are carried out at room temperature in a buffer that more resembles the physiological cellular environment (100 mM KCl, with 1 mM $MgCl_2$). The Mg^{2+} is needed to activate the Ca^{2+} pump. Following active accumulation of Ca^{2+} by the Ca^{2+} pump, 1,4NQ was added to stimulate the Ca^{2+} release mechanism. The Ca^{2+} release assays occurred over a period of a few minutes. It is highly unlikely that the phase 2 inhibition observed in the binding assay would influence the initial rate of Ca^{2+} release from actively loaded SR vesicles, as reported in Fig. 13, where 2mM GSH totally inhibited 1,4NQ induced Ca^{2+} release, pretreatment with GSH only partially inhibited ryanodine binding stimulated by 1,4NQ. Due primarily to the long time period over which the binding assay is carried out, and the specificity of the binding assay, subtle small changes in ryanodine binding are much more easily observed than are changes in Ca^{2+} effluxes.

The overall results strongly support a theory in which at least two or three critical thiols, located at different sites on the RyR, are functionally involved in the regulation of channel operation through a redox mechanism. This theory is in agreement with the hypothese of Aghdasi et al., 1997. They recognized three distinct phases related to three functional classes of sulfhydryls on the CRC. In addition, they suggested that the class of sulfhydryl groups which was selectively inhibited by the alkylating reagent N-ethylmaleimide (NEM) and activated by the sulfhydryl oxidizing reagent diamide, was located at a channel activation site. This thiol functionally controlled the activation of the channel. Alkylation of this thiol by NEM led to a conformational change in the channel protein, and a loss in its ability to activate the channel. Pretreatment of the thiol with diamide protected it from alkylation ,thereby activating the channel.

The question remaining is how the critical thiols function to control channel gating. Inconsistent results have emerged from different research groups. Pessah's research group claimed that a disulfide cross-linking occurred between a subunit of the RyR and the adjacent protein triadin when the Ca^{2+} release channel was activated (Liu et al., 1995). Recently, evidence was provided by Hamilton's group for a disulfide cross-linkage between two subunits on the RyR when the Ca^{2+} release channel was activated by oxidation. There is no further evidence to distinguish which of these two groups is correct. However it does seem clear that the Ca^{2+} release channel is modulated by oxidation-reduction mechanisms during the opening and closing of the

CRC. The hyperreactive thiol groups on the RyR play a key role in the activation of the CRC when they are oxidized to form disulfides, and in the closing of the CRC when they are reduced. The data presented in this thesis demonstrate that there are at least two distinct functional thiols at different locations on the RyR. They are characterized as activation thiols (ASH) and inhibition thiols (ISH). The ASHs are located at activation sites that open the channel when they are oxidized, by forming disulfides. The ISHs are located at inhibitory sites that close the channel when they are oxidized, regardless of the state of the ASHs. Further research is needed to describe the role of the intracellular redox environment in the control of SR Ca^{2+} release channel gating and its influence on muscle contraction.

Bibliography

Abramson, J. J., Trimm, J. L., Weden, L. and Salama, G. 1983. Heavy metals induce calcium release from sarcoplasmic reticulum vesicles isolated from skeletal muscle. *Proc. Natl. Acad. Sci.* **80,** 1526-1530.

Abramson, J. J., Buck, E., Salama, G., Casida, J. E., and Pessah, I. N. 1988. Mechanism of Anthraquinone-induced Calcium Release form Skeletal Muscle SR . *J. Biol. Chem.* **263,** 18750-18758

Anderson, K. and Meissner, G. 1995. T-tubule depolarization-induced SR Ca^{2+} release is controlled by dihydropyridine receptor- and Ca^{2+} -dependent mechanisms in cell homogenates from rabbit skeletal muscle. *J. Gen. Physiol.* **105,** 363-383

Affolter, H, and E. Carafoli. The Ca^{2+}- Na^{+} antiporter of heart mitochondria operates electroneutrally. *Biochem. Biophys. Res. Commun.* 95:193-196,1980

Aghdasi, B., Zhang, J. Z., Wu, Y., Reid, M. B., Hamilton, S. L. Multiple classes of sulfhydryls modulate the skeletal muscle Ca^{2+} release channel. 1997, *J. Bio. Chem.* 272,3739-3748.

Bourguignon, L. Y., Jin, H., Linda, N., Brandel , N. R., and Zhang, S. H. 1993. The involvement of ankyrin in the regulation of inositol 1,4,5-trisphosphate

receptor -mediated in internal Ca^{2+} release from Ca^{2+} storage vesicles in mouse T-lymphoma cells. *J. Biol. Chem.* 268, 7290-7297.

Carl, S. L., Felix, K., Caswell, A. H., Brand, N. R., Brunschwig, J. P., 1995. Immunolocalization of Triadin, DHP Receptors and the Ryanodine Receptors in Adult and Developing Skeletal Muscle of Rats. *Muscle-Nerve*. **18(11)**, 1232-1243

Chance. B., Legallais, V., Sorge, J., and Graham. N. 1975. A versatile time-sharing multichannel spectrophotometer, reflectometer, and fluorometer. *Anal. Biochem.* **66,** 498-564

Clark, W. M. Oxidation Reduction Potentials of Organic System, *Williams & Wilkins*, Baltimore, Maryland, 1960

Chu, A. and Stefani, E. 1991. Phosphatidyl 4,5-bisphosphate-induced Ca^{2+} release from skeletal muscle sarcoplaasmic reticulum terminal cisternal membranes. Ca^{2+} flux and single channel studies. *J. Biol. Chem.* **266,** 7699-7705.

Cohen, G. M., Wilson, G. D., Gibby, E. M., Smith, M. T. d'Arcy Doherty, M and Connors, T. A 1983. 1-Naphthol selective antitumour agent. *Biochem. Pharmacol.* **32,** 2363-2365.

Daglish, C. 1950. The ultraviolet absorption spectra of some hydroxynapththalenes. *J. Am. Chem. Soc.* **72,** 4859-4864.

d'Arcy Doherty, M., Cohen, G. M. and Smith, M. T. 1984. Mechanisms of toxic injury to isolated hepatocytes by 1-naphthol. *Biochem. Pharmacol.* **33,** 543-549.

Dulhunty, A. F. Junankar, P. R., Eager, K. R., Ahern, G. P., and Laver, C. R. 1996, Ion channels in the sarcopasmic reticulum of striated muscle. *Acta Phy. Scand.* **156,** 375-385.

Favero, T. G., Zable, A. C., and Abramson, J. J. 1995. Hydrogen peroxide stimulates the Ca^{2+} release channel from skeletal muscle sarcoplasmic reticulum. *J. Biol. Chem.* **270**, 25557-25563

Flucher, B. E., Andrews, S. B., Fleischer, S., Marks, A. R., Caswell, A. Triad formation: organization and triadin in normal and dysgenic muscle in vitro. *J. Cell. Biol.* 1993, **123(5)**, 1161-1174

Guo, W. Jorgenson, A. O., Jones, L. R., and Campbell. K. P.1996. Biochemical characterization and molecular cloning of cardiac triadin. *J. Biol. Chem.* **271**, 458-465.

Hasegawa, T. and Kumagai, S. 1989. A G-protein of sarcoplasmic reticulum of skeletal muscle is activated by caffeine or inositol triphosphate. *FEBS Letters.* **244,** 283-289.

Hill, A. W. 1910. The possible effects of the aggregation of the molecules of hemoglobin on its dissociation curves. *J. Physiol.* **40,** iv-vii.

Hirayama, Kenzo, 1971. *Handbook of Ultraviolet and Visible Absorption Spectra of Organic Compounds.* Odawara, Japan. 260.

Howell, J.N. 1969 *J.Phys.* (London) **201**, 515-533.

Jayaraman, T., A.M. Brillantes, A.P.Timerman, S. Fleischer, H. Erdjumen P. Tempst, and A. R. Marks. 1992. FK506 binding protein associated calcium release channel (ryanodine receptor). *J.Biol. Chem.* **267,** 9474-9

Kalckar, . M. 1947. Differential spectrophotometry of purine compounds by means of specific enzymes. *J. Biol. Chem.* **167,** 461-475.

Kappusl, H. and Sies, H. 1981. Toxic drug effects associated with oxygen metabolism: redox cycling and lipid peroxidation. *Experimentia* **37,** 1233-1241.

Knudson, C. M., Strong , K. K., Moomaw, C. R., Slaughter, C. A.,1993. Primary structure topologicalanalysis of junctional sarcoplasmic reticulum glycoprotein (triadin). *J. Biol. Chem.* **268**, 12646-12654 .

Lai, F. A., Erickson, H. P., Rousseau. E., Liu, Q. Y., and Meissner, G. 1988. Purification and reconstutution of the calcium release channel from skeletal muscle. *Nature*. **331,** 315-319.

Lai, F. A., Misra, M., Xu, L., Smith, A. and Meissner, G. 1989. The ryanodine receptor-Ca^{2+} release channel complex of skeletal muscle sarcoplasmic reticulum. *J. Biol. Chem.* **264,** 16776-16785.

Lind, C., Hochstein, P. and Erster, L. 1982. DT-diaphonase as a quinone reductase: a cellular control device against semiquinone and superoxide radical formation. *Arch. Biochem. Biophys.* **190,** 97-108.

Liu, G., Abramson, J. J., Zable, A. C., and Pessah, I. N. 1994. Direct Evidence for the Existence and Functional Role of Hyperreactive Sulfhydryls on the RyR-

Triadin complex Selectively Labeled by Coumarin Maleimide 7-diethylamino-3-(4'maleimidylphenyl)-4-methylcoumarin *Molecular Pharamcology*, **45**,189-200.

Liu, G., and Pessah, I. N. 1994. Molecular interaction between ryanodine receptor and glycoprotein triadin involves redox cycling of functionally important hyperreactive sulfhydryls. *J. Biol. Chem.* **269**,6511-6516.

Lu, X., Xu, L. and Meissner, G. 1994. Activation of the skeletal muscle calcium release channel by a cytoplasmic loop of the dihydropyridine receptor. *J. Biol. Chem.* **269,** 6511-6516.

MacLennan, D. H. 1970. Purification and properties of an adenosine triphosphatase from sarcoplasmic reticulum. *J. Biol. Chem.* **245**, 4508-4518.

McMahon, S., Stern, A., The interrelationship of Superoxide Dismutase and Peroxidatic Enzymes in the Red Cell. 1979 *Biochim. et Biophsica Acta*, **566** 253-258.

Meissner, G., Darling, E., and Eveleth, J. 1986. Kinetics of rapid Ca^{2+} release by sarcoplasmic reticulum. Effects of Ca^{2+}, Mg^{2+}, and adenine nucleotides. *Biochemistry*. **25,** 236-244.

Mickelson, J. R., Gallant, E. M., Litterer, L. A., Johnson, K. M., Rempel, W. E., and Louis, C. F. 1988, *J. Biol. Chem.* **263**, 9310-9315.

Moore, L., Davenport, G. R. and Landon, E. J. 1976. Calcium uptake of a rat liver microsomal subcellular fraction in response to in vivo administration of carbon tetrachloride. *J. Biol. Chem.* **251,** 1197-1201.

Morton, R.A. The Biochemistry of Quinones, Academic Press, London and New York, 1965.

Ohnishi, S.T. 1979. Calcium-induced calcium from fragmented sarcoplasmic reticulum. *J. Biochem.* **86,** 1147-1150.

Orlova, E.V., I. 1996.Two structural configurations of the skeletal muscle calcium release channel. *Nature struct. Biol.* **3**,547-552.

Pessah, I. N., Stambuk, R. A., Casida, J. E. 1986, Ca^{2+}-activated Ryanodine Binding: Mechanisms of Sensitivity and Intensity Modulation by Mg^{2+}, Caffeine, and Adenine Nucleotides. *Mol. Pharmacol.* **31**, 232-238.

Powis, G., Svingen, B. A. and Appel, P. 1981. Quinone-stimulated superoxide formation by subcellalar fractions, isolated hepatocytes, and other cells. *J. Cell Biol.* **81,** 592-607.

Quinn, K.E.,and Ehrlich, B. E. 1996, Methanethiosulfonate derivatives inhibit current through the ryanodine receptor/channel. *Biophys. J.* 70, A389 (abstr.).

Radermacher, M., Grassucci, R., Frank, J., Timerman, A, P., Fleischer, S, & Wagenknecht, T. 1994. Cryo-electron microscpy and three-dimentional reconstruction of the calcium release channel/ryanodine receptor from skeletal muscle. *J Cell Biol* **127,** 411-423.

Salama, G. and Abramson, J. J., 1984. Silver ions trigger Ca^{2+} release by acting at the apparent physiological release site in sarcoplasmic reticulum. *J. Biol. Chem.* **259,** 13363-13369.

Smith, J. S., Coronado, R. and Meissner, G. 1986. Single Channel measurements of the calcium release channel from skeletal muscle sarcoplasmic reticulum: Activation by Ca^{2+} and ATP and modulation by Mg^{2+}. *J. Gen. Physiol*, **88**, 573-588.

Smith, M. T., Evans, C.G., Thor, H., Orrenivs. S., Quinone-Induced Oxidation Injury to Cells and Tissues. Oxidative Stress. *Academic Press* 1985, 91-113.

Stuart, J., Pessah, I.N., Favero, T.G. and Abramson, J. J. 1992. Photooxidation of skeletal muscle sarcoplasmic reticulum. *Arch. Biochem. Biophys.* **292**, 512-521.

Suematsu, E., Hirata, M., Sasaguri, T., Hashimoto, T., and Kuriyama, H. 1985. Roles of Ca^{2+} on the inositol 1,4,5-triphosphate-induced release of Ca^{2+} from saponin -permeabilized single cells of the porcine coronary artery. *Comp. Biochem. Physiol.* 82, 645-649.

Takeshima, H., Nishimura, S., Matsumoto, T., Ishida, H., Kangawa, K., Minamino, N., Matsuo, H., Masamichi, U., Hanoaka, M., Hirose, T., and Numa, S. 1989. Primary structure and expression from complementary DNA of skeletal muscle ryanodine receptor. *Nature* **339**, 439-445.

Talcott, R. E., Smith, M. T., and Giannini, K. K. 1985. Inhibition of microsomal lipid peroxidation by naphthoquinones: structure-activity relationships and possible mechanisms of action. *Chem. -Biol. Interact.* **19,** 265-278.

Thor, H., Smith, M. T., Hartzell, P., Bellomo, G., Jewell, S. A. and Orrenius, S. 1982. The metabolism of menadione (2-methyl-1,4-naphthoquinone) by isolated hepatocytes. A study of the implications of oxidative stress in intact cells. *J. Biol. Chem.* **257,** 12419-12425.

Timerman, A. P., E. Ogunbumni, E. Freund, G. Wiederrecht, A. R. Marks, and S. Fleischer. 1993. The calcium release channel of sarcoplasmic reticulum is modulated by FK-506- binding protein. Dissociation and reconstitution of the FKBP12 to the calcium release channel of skeletal muscle sarcoplasmic reticulum. *J. Biol. chem.* **268**:22,992-22,999.

Trimm, J. L., Salama, G. and Abramson, J. J. 1986. Sulfhydryl oxidation induces rapid calcium release from sarcoplasmic reticulum vesicles. *J. Biol. Chem.* **261,** 16092-16098.

Voet, D., Voet, J. G., 1990 *Biochemistry* by John Wiley & Sons, Inc.

Wefers, H. and Sies, H. 1983. Hepatic low-level chemiluminescence during redox cycling of menadione and the menadione-glutathione conjugate: relation to glutathione and NAD(P)H: quinone reductase (DT-diaphorase) activity. *Arch. Biochem. Biophys.* **224,** 568-578.

Xiong, H. Buck, E., Stuart, J., Pessah, I. N. Salama, G. and Abramson, J. J. 1992. Rose bengal activates the Ca^{2+} release channel from skeletal muscle sarcoplasmic reticulum. *Arch. Biochem. Biophys.* **292**, 522-528.

Zable, A.C., Favero, T. G., Abramson, J. J., Glutathione Modulates Ryanodine Receptor from Skeletal Muscle Sarcoplasmic Reticulum. 1997, *J. Biol. Chem.* **272**, 7069-7077.

APPENDIX:

List of abbreviations

Chapter 1: Introduction

SR, sarcoplasmic reticulum; T-tubules, transverse tubules; DHPR, dihydropyridine receptor; RyR, Ca^{2+} release channel; ATP, adenosine 5'-triposphate; SL, sarcolemma; ER, endoplasmic reticulum; EC coupling, excitation-contraction coupling; LSR, longitudinal SR; TC, terminal cisternae; CRC, Ca^{2+} release channel; JFP, junctional-foot-protein; FKBP-12, 12 kDa FK506 binding protein; CSR, cisternae SR; CPM, coumaryl maleimide; HMWC, high molecular weight complex; IP_3, inositol 1,4,5-triphosphate; PIP_2, phosphatidylinositol 4,5-bisphosphate; GSSG, glutathione; GSH, reduced glutathione; DTT, dithiothreitol.

Chapter 2: General Methods

SR, sarcoplasmic reticulum; DTT, dithiothreitol; Hepes, 4-(2-hydroxyethyl)-1-piperazineethanesulfonic acid; APIII, antipyralazo III; RR, ruthenium red; CP, creatine phosphate; CPK, creatine phosphokinase; EGTA, ethyleneglycol-bis-(β-aminoethyl ether) N,N,N',N'-tetracetic acid; 1,4NQ, 1,4-naphthoquinone; 1,2NQ, 1,2-naphthoquinone; 1,4NQ-2-S, 1,4-naphthoquinone-2-sulfonate; A2S, anthraquinone-2-sulfonate; B_{max}, maximal ryanodine bound; *n*, Hill constant; K_d, equilibrium dissociation constant; CRC, Ca^{2+} release channel; RyR, Ca^{2+} release chanel; k_{+1}, association rate

constant; k_{-1}, dissociation rate constant; K, observed association constant; EC_{50}, concentration necessary to elicit 50% inhibition.

Chapter 3: Spectrophotometric Assay of 1,4-Naphthoquinone Stimulating Ca^{2+} Efflux

SR, sarcoplasmic reticulum; RyR, Ca^{2+} release chanel; DTT, dithiothreitol; Hepes, 4-(2-hydroxyethyl)-1-piperazineethanesulfonic acid; APIII, antipyralazo III; RR, ruthenium red; CP, creatine phosphate; CPK, creatine phosphokinase; GSH, reduced glutathione; SOD, Superoxide dismutase; H_2O_2, hydrogen peroxide.

Chapter 4: Equilibrium Ryanodine Binding Assay

SR, sarcoplasmic reticulum; RyR, Ca^{2+} release chanel; DTT, dithiothreitol; GSH, reduced glutathione; Hepes, 4-(2-hydroxyethyl)-1-piperazineethanesulfonic acid; 1,4NQ, 1,4-naphthoquinone; 1,2NQ, 1,2- naphthoquinone; 1,4NQ-2-S, 1,4-naphthoquinone-2-sulfonate; B_{max}, maximal ryanodine bound; n, Hill constant; K_d, equilibrium dissociation constant; CRC, Ca^{2+} release channel; EC_{50}, concentration necessary to elicit 50% inhibition.

Chapter 5: Dynamic Ryanodine Binding Assay

SR, sarcoplasmic reticulum; RyR, Ca^{2+} release chanel; DTT, dithiothreitol; GSH, reduced glutathione; Hepes, 4-(2-hydroxyethyl)-1-piperazineethanesulfonic acid;

1,4NQ, 1,4-naphthoquinone; CRC, Ca^{2+} release channel; k_{+1}, association rate constant; k_{-1}, dissociation rate constant; *K*, observed association constant.

Chapter 6: Conclusions and Discussion

SR, sarcoplasmic reticulum; DTT, dithiothreitol; CRC, Ca^{2+} release channel; RyR, Ca^{2+} release chanel; 1,4NQ, 1,4-naphthoquinone; GSH, reduced glutathione; *n*, Hill constant; K_d, equilibrium dissociation constant; B_{max}, maximal ryanodine bound; EC_{50}, concentration necessary to elicit 50% inhibition; k_{+1}, association rate constant; k_{-1}, dissociation rate constant; ASH, activation thiol; ISH, inhibition thiol.